USGS
science for a changing world

An Analysis of the Potential for Glen Canyon Dam Releases to Inundate Archaeological Sites in the Grand Canyon, Arizona

Open-File Report 2014–1193

U.S. Department of the Interior
U.S. Geological Survey

Cover: View of the Colorado River and its left bank at river mile 72.7, looking north from Unkar Delta. Photograph taken by A. East, U.S. Geological Survey, May 3, 2013.

An Analysis of the Potential for Glen Canyon Dam Releases to Inundate Archaeological Sites in the Grand Canyon, Arizona

By Hoda A. Sondossi and Helen C. Fairley

Open-File Report 2014–1193

U.S. Department of the Interior
U.S. Geological Survey

U.S. Department of the Interior
SALLY JEWELL, Secretary

U.S. Geological Survey
Suzette Kimball, Acting Director

U.S. Geological Survey, Reston, Virginia: 2014

Suggested citation:
Sondossi, H.A., and Fairley, H.C., 2014, An analysis of the potential for Glen Canyon Dam releases to inundate archaeological sites in the Grand Canyon, Arizona: U.S. Geological Survey Open-File Report 2014-1193, 26 p., *http://dx.doi.org/10.3133/ofr20141193*.

ISSN 2331-1258 (online)

Contents

Figures

Tables

Conversion Factors and Datums

Conversion Factors

Inch/Pound to SI

Multiply	By	To obtain
	Length	
mile (mi)	1.609	kilometer (km)
	Flow rate	
cubic foot per second (ft^3/s)	0.02832	cubic meter per second (m^3/s)

SI to Inch/Pound

Multiply	By	To obtain
	Length	
meter (m)	3.281	foot (ft)
kilometer (km)	0.6214	mile (mi)
	Area	
square meter (m^2)	0.0002471	acre
square meter (m^2)	10.76	square foot (ft^2)
	Flow rate	
cubic meter per second (m^3/s)	35.31	cubic foot per second (ft^3/s)

Datums

Vertical coordinate information is referenced to the North American Vertical Datum of 1988 (NAVD 88)
Horizontal coordinate information is referenced North American Datum of 1983 (NAD 83)
Elevation, as used in this report, refers to distance above the vertical datum.

An Analysis of the Potential for Glen Canyon Dam Releases to Inundate Archaeological Sites in the Grand Canyon, Arizona

By Hoda A. Sondossi[1] and Helen C. Fairley[2]

Abstract

The development of a one-dimensional flow-routing model for the Colorado River between Lees Ferry and Diamond Creek, Arizona in 2008 provided a potentially useful tool for assessing the degree to which varying discharges from Glen Canyon Dam may inundate terrestrial environments and potentially affect resources located within the zone of inundation. Using outputs from the model, a geographic information system analysis was completed to evaluate the degree to which flows from Glen Canyon Dam might inundate archaeological sites located along the Colorado River in the Grand Canyon. The analysis indicates that between 4 and 19 sites could be partially inundated by flows released from Glen Canyon Dam under current (2014) operating guidelines, and as many as 82 archaeological sites may have been inundated to varying degrees by uncontrolled high flows released in June 1983. Additionally, the analysis indicates that more of the sites currently (2014) proposed for active management by the National Park Service are located at low elevations and, therefore, tend to be more susceptible to potential inundation effects than sites not currently (2014) targeted for management actions, although the potential for inundation occurs in both groups of sites. Because of several potential sources of error and uncertainty associated with the model and with limitations of the archaeological data used in this analysis, the results are not unequivocal. These caveats, along with the fact that dam-related impacts can involve more than surface-inundation effects, suggest that the results of this analysis should be used with caution to infer potential effects of Glen Canyon Dam on archaeological sites in the Grand Canyon.

Introduction

For more than two decades, research has been done by various Federal agencies and cooperating scientists to improve the understanding of how varying releases from Glen Canyon Dam interact with and affect downstream aquatic and shoreline resources (Gloss and others, 2005). One category of shoreline resources is the numerous archaeological sites situated on and in alluvial deposits derived from the Colorado River (Fairley and others, 1994; Fairley, 2003). These archaeological sites range in age from more than 8,000 years before present to the mid-20th century, and include masonry structures, inscriptions, scatters of artifacts, roasting pits, and various other physical remains representing the past 8,000 years of human use and occupation along the banks of the Colorado River.

[1]U.S. Fish and Wildlife Service (previously with the U.S. Geological Survey).
[2]U.S. Geological Survey.

National Park Service (NPS) managers and archaeologists have known for some time that some archaeological sites are located within areas inundated by past floods and pre-dam-controlled releases, and that some sites have been partially preserved through burial by prehistorical and historical flood deposits (Hereford and others, 1993, 1996; Draut and other, 2005); however, the precise number of archaeological sites occurring within areas previously inundated by past floods or located within the area of potential inundation from dam-controlled flows was previously unknown.

Prior to 2008, a significant limitation to resolving the controversy about the relation between archaeological sites and potential for inundation by river flows was the lack of a system-wide stage-discharge model capable of accurately predicting the elevation of streamflow reached by historical floods and the flow regime typically released through Glen Canyon Dam. In 2008, a one-dimensional flow-routing model was developed and published by Magirl and others (2008). The original intent for developing this model was to analyze how tributary debris flows and main stem floods have interacted over the past several centuries, resulting in channel incision and (or) aggradation at particular places in the Colorado River corridor of the Grand Canyon (C.S. Magirl, U.S. Geological Survey, oral commun., 2009). Managers and stakeholders involved in the Glen Canyon Dam Adaptive Management Program (GCDAMP) quickly recognized the potential applicability of this model for a wide variety of other research purposes, such as analyzing potential inundation of terrestrial habitats under varying flow regimes. Soon after the model was published, GCDAMP stakeholders requested that the U.S. Geological Survey (USGS) undertake an analysis to identify archaeological sites with the highest potential to be directly affected by dam operations through inundation.

In response to this request, the Grand Canyon Monitoring and Research Center (GCMRC) staff conducted a geographic information system (GIS) analysis to determine how various releases from Glen Canyon Dam, as well as historical (or future) uncontrolled flood events, might inundate, and thereby affect, downstream archaeological sites in the Grand Canyon. One objective of this analysis was to develop flow-based criteria for prioritizing archaeological sites for future treatment, monitoring and other management purposes. A second objective was to clarify the extent to which past flood events may have affected these archaeological resources. This analysis involved a comparison of predicted water-surface elevations (stages) associated with six discrete discharges (708 m^3/s [25,000 ft^3/s]; 1,274 m^3/s [45,000 ft^3/s]; 2,747 m^3/s [97,000 ft^3/s]; 3,540 m^3/s [125,000 ft^3/s]; 4,814 m^3/s [170,000 ft^3/s]; and 5,947 m^3/s [210,000 ft^3/s]) to ground-surface elevations within cultural sites located along the Colorado River, in order to determine the likelihood and possible extent of inundation. The six discharges reflect the maximum stage of the three highest pre-dam floods (Topping and others, 2003), plus three important discharge levels of the post-dam era (U.S. Department of the Interior, 1995, 1996; Melis, 2011). Three different GIS analyses were conducted to evaluate the potential for inundation under these six discharges. In this report, we briefly describe each of these analyses and explain the usefulness and limitations of each set of results; however, this report focuses primarily on the results of the third analysis, which incorporates estimated ranges of uncertainty associated with each of the modeled stage elevation projections.

Study Area

The focus of this analysis is on the Colorado River corridor between Lees Ferry, near the mouth of the Paria River, and the confluence of Diamond Creek (fig. 1), a distance of approximately 364 km (226 mi). Glen Canyon Dam is about 25 km (15.5 mi) upstream of Lees Ferry. The one-dimensional flow-routing model developed by Magirl and others (2008) does not include the section of the river corridor upstream of Lees Ferry, nor does it extend downstream of Diamond Creek (Magirl and others, 2008).

The study area includes most, but not all, of the archaeological sites located in the area potentially affected by past and current river flows between Lees Ferry and Diamond Creek, as documented by Fairley and others (1994) during the 1990–91 inventory of the 410-km (255-mi) long Colorado River corridor between Glen Canyon Dam and Separation Canyon, near the head of Lake Mead. A total of 283 archaeological sites were recorded in this inventory in the presumed area of potential effects from dam operations downstream of Lees Ferry. Location information for 242 of these 283 sites was provided by the NPS for this analysis in the form of either GIS polygons or Universal Transverse Mercator (UTM) coordinates. In keeping with U.S. Department of the Interior policy, precise archaeological site locations are not disclosed in this report, but are on record with the NPS, Grand Canyon National Park, Division of Science and Resource Management, at Grand Canyon, Arizona.

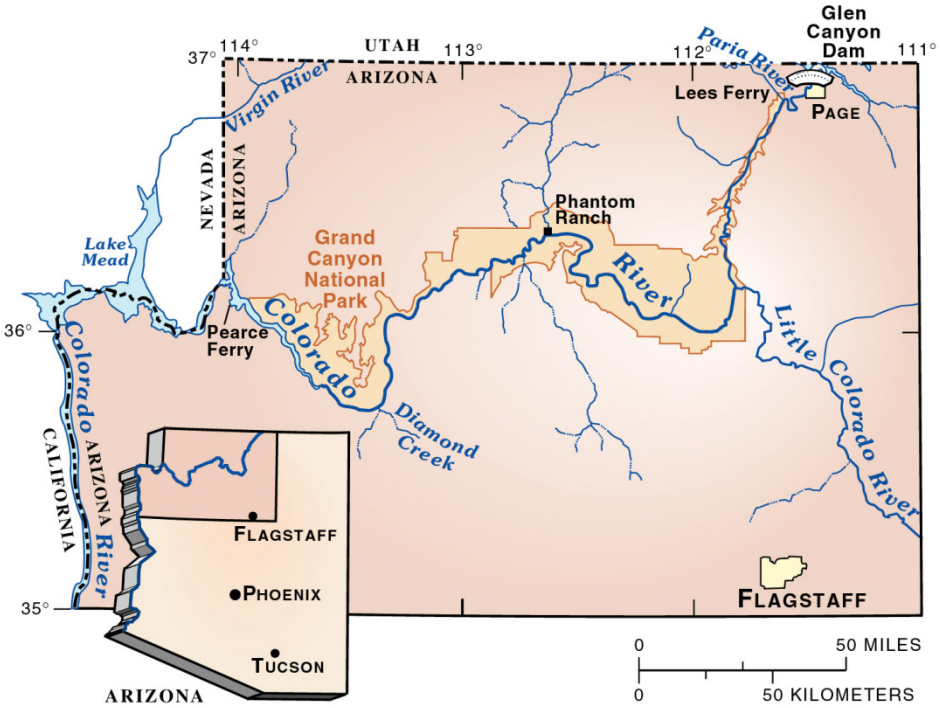

Figure 1. Map showing project area, located in the Colorado River corridor between Lees Ferry and Diamond Creek, Grand Canyon National Park, Arizona.

Methods

Using the six "virtual shorelines" developed by Magirl and others (2008), an initial GIS analysis was conducted as a basic assessment of the potential of the Colorado River to inundate cultural sites in the Grand Canyon at the six discharges listed in the introduction. (Metric values of these six discharges are rounded throughout the remainder of this report, as follows: 700 m^3/s [25,000 ft^3/s]; 1,270 m^3/s [45,000 ft^3/s]; 2,750 m^3/s [97,000 ft^3/s]; 3,500 m^3/s [125,000 ft^3/s]; 4,800 m^3/s [170,000 ft^3/s]; 5,900 m^3/s [210,000 ft^3/s]). This initial analysis did not account for the uncertainty (as discussed by Magirl and others, 2008) associated with the predicted stages. A subsequent GIS analysis was limited to only the area within the boundaries of the cultural sites. This second analysis is referred to hereinafter as the "restricted raster analysis." In the third analysis, the steps Magirl and others (2008) took to generate "virtual shorelines" were repeated to generate additional water-surface polygons representing the upper and lower bounds of error for each of the six modeled discharges, as previously defined by Magirl and others (2008). The resulting GIS water-surface polygons then were used to analyze the likelihood of inundation at the 242 archaeological sites in relation to the full range of possible error associated with each of the modeled discharges. In this report, we present the results of the final canyon-wide analysis and explain the differences between the results of this analysis and the restricted raster analysis.

Source Data

The following spatial datasets were used in this analysis:

1. Unpublished cultural site boundary data (vector: polygons). Source: NPS, Grand Canyon National Park, Division of Science and Resource Management, supplemented with unpublished spatial point data provided by G. O'Brien and J. Pederson, Department of Geology, Utah State University.
2. Water-surface elevation (raster: grids). Source: USGS, GCMRC. Unpublished data developed by M. Breedlove and H. Sondossi, GCMRC.
3. Topography (raster: grids). Source: USGS, GCMRC. Unpublished digital surface-elevation data developed by ISTAR America, Inc., under contract to GCMRC.
4. Virtual shorelines (vector: polygons), representing the intersection of water-surface elevations with canyon topography between Lees Ferry and Diamond Creek. Published data developed by Magirl and others (2008) and unpublished data developed by H.A. Sondossi. Source: USGS, GCMRC.

The same source data were used for all analyses involving virtual shorelines and cultural sites. In the following sections, each of these data sources is described in more detail

Cultural Site Data

Spatial data, in vector (polygon) format, from 242 archaeological sites were used for this analysis. These 242 sites included 161 sites that have been identified by the Bureau of Reclamation and the NPS as potential candidates for future excavation or other forms of management "treatment" such as erosion control (Damp and others, 2007), along with an additional 81 sites not currently slated for treatment but considered sensitive to potential adverse effects from present and future dam operations (O'Brien and Pederson, 2009).

Digital polygon data delineating the areas occupied by 232 of the cultural sites used in this analysis were generated and provided to the GCMRC by the NPS. No polygon data existed for 10 of the cultural sites. However, point data (in UTM coordinates) for these 10 sites had been created prior to this study for the purposes of completing a geomorphic assessment of the stability at these sites (O'Brien and Pederson, 2009). These coordinates were used as centroids to generate circular buffer polygons (using the "buffer" command in the Environmental Systems Research Institute, Inc. [ESRI] ArcMap™ program) with a 4-m diameter. The exact extent of at least two of these cultural sites is known to be larger than the artificial circles generated by this method.

The 242 sites were partitioned and analyzed as two separate groups—Groups A and B:

1. Group A consisted of 151 sites that had been identified as candidates for future treatment (Damp and others, 2007) plus 10 sites identified for excavation by the Museum of Northern Arizona (total of 161 sites).
2. Group B included other sites potentially affected by dam operations (81 sites).

Three sites in Group A and two sites in Group B subsequently were determined to be downstream of Diamond Creek, beyond the geographical extent of the flow-routing model; therefore, these five sites were not included in the final analysis.

Basic summary statistics pertaining to the size distribution of the two sets of cultural sites are shown in table 1. The two groups of cultural sites differ in overall range of size distribution, as well as in the arithmetic mean and median. These differences have a bearing on the likelihood of inundation.

Table 1. Summary statistics for the two cultural site datasets (Groups A and B), Colorado River corridor between Lees Ferry and Diamond Creek, Grand Canyon National Park, Arizona.

[m^2, square meter]

Cultural site area and site count	Group A	Group B
Total area of all sites (m^2)	386,400	87,717
Site count	158	79
Mean site area (m^2)	2,440.9	1,110.3
Median site area (m^2)	808.5	313
Maximum site area (m^2)	42,170	13,346
Minimum site area (m^2)	6	5

Modeled Water-Surface Elevation Data

Water-surface elevations associated with the six different discharges initially were modeled for the 364 km (about 226 mi) between Lees Ferry and Diamond Creek (fig. 1) as part of the Magirl and others (2008) study. The lowest discharge (700 m^3/s [25,000 ft^3/s]) represents the maximum release level from Glen Canyon Dam currently permitted under normal operating criteria of the Modified Low Fluctuating Flow regime (U.S Department of the Interior, 1996). The second-lowest discharge (1,270 m^3/s [45,000 ft^3/s]) represents the maximum level possible for experimental flood releases, when all turbines in Glen Canyon Dam are fully operational and the jet tubes are operating simultaneously at full capacity (Melis, 2011). The third-lowest discharge (2,750 m^3/s [97,000 ft^3/s]) represents the maximum post-dam discharge that occurred in June 1983, as a result of an uncontrolled release of excess water from Lake Powell. The three highest discharges (3,500 m^3/s [125,000 ft^3/s], 4,800 m^3/s [170,000 ft^3/s], and 5,900 m^3/s [210,000 ft^3/s]) are the maximum flows of pre-dam spring floods in 1957, 1921, and 1884, respectively, as calculated by Topping and others (2003). For the final analysis, additional water-surface polygons representing the upper and lower bounds of each of the six discharges were created following the same GIS methods used to create the original six water-surface polygons described in Magirl and others (2008).

Topography

Terrestrial surface topography was derived from aerial imagery collected by ISTAR™ America, Inc., under contract to the GCMRC during a May 2002 overflight of the same above-mentioned extent of the Grand Canyon. Automated digital photogrammetry, with an accuracy of ±0.3 m (Davis, 2004), was used to create a 1-m digital surface model (DSM) for the entire river corridor.

Virtual Shorelines

Virtual shorelines are shoreline projections created by intersecting modeled surface-water elevations with three-dimensional terrain models representing the topography of the river corridor. Magirl and others (2008) generated the original set of virtual shorelines using topographic data and modeled water-surface elevations developed specifically for the Colorado River in the Grand Canyon. As noted in the "Topography" section above, the primary source of topographic data was a 1-m resolution DSM derived from ISTAR™-automated digital photogrammetry collected in 2002, with an accuracy of ±0.3 m (Davis, 2004). Magirl and others (2008) used these DSMs to generate 2,680 cross sections along the length of the Colorado River between Lees Ferry and Diamond Creek (fig. 1). These cross sections relied on the topography derived from the 2002 DSM to define channel geometry above the 227 m^3/s discharge level; below this level, channel geometry was created synthetically, based on assumptions about typical cross-sectional form in varying geomorphic contexts (Magirl and others, 2008), unless more detailed and accurate data existed from local surveys (for example, Hazel and others, 2006). The cross sections were used to model water-surface elevations using the one-dimensional modeling system originally developed by Magirl (2006), which is based on the Hydrologic Engineering Center River Analysis System (HEC-RAS) software application (Version 3.1), designed by the U.S. Army Corps of Engineers (Brunner, 2002). HEC-RAS is a "standard step" model used in this case to predict water-surface elevation (stage) associated with various discharges using parameters such as cross-section geometry, flow velocity, and local slope (fig. 2).

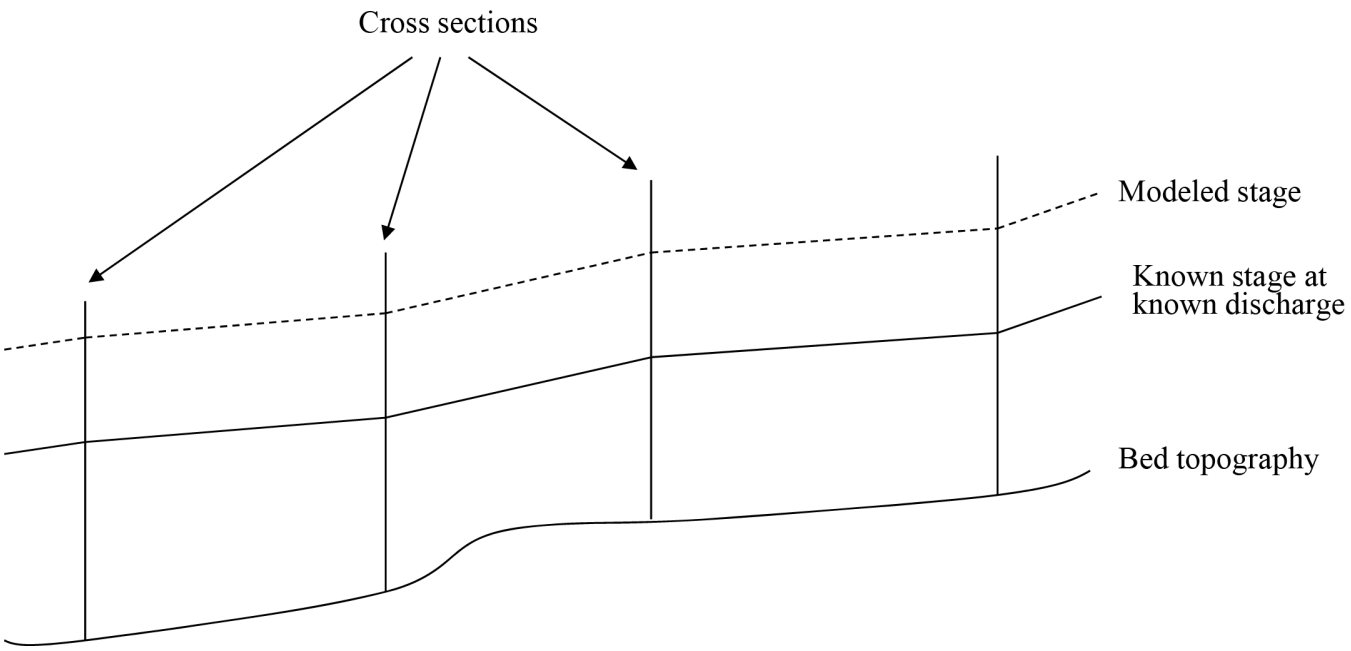

Figure 2. Diagram showing longitudinal profile and cross sections similar to those used to generate virtual shorelines.

Magirl and others (2008) used the 2,680 cross sections to generate water-surface elevation grids for each modeled discharge. To create these cross sections, a line (vector) layer of the Colorado River channel centerline first was generated, and from this centerline, perpendicular lines were extended in either direction at the designated locations of the 2,680 cross sections (fig. 3). Cross-section locations were selected by Magirl and others (2008) based on recommendations in the hydraulic literature (Benson and Dalrymple, 1967; Davidian, 1984; Randle and Pemberton, 1987) to capture the fall of the water surface at rapids and outside of eddies. For each modeled discharge, these cross-section lines were attributed with elevations in real-world coordinates for water-surface elevations at that discharge. Elevation values between each pair of cross sections were interpolated by essentially connecting them with a straight line in three-dimensional space (figs. 2 and 3). The three-dimensional data were used to generate canyon-wide 1-m resolution grids (raster layers) of water-surface elevation for the modeled discharges.

In order to generate the virtual shorelines, Magirl and others (2008) compared the generated water-surface elevation layers to the topography layer in raster format using the "subtract" command in ArcGrid™, the raster analysis module within ARC/Info™. This generated a third raster layer with areas of positive and negative "difference" values (fig. 4). Next, the "Gridpoly" command was used in Arc/Info™ to generate polygons separating areas of positive value from areas of negative value. These polygons are the virtual shoreline polygon layers. The various steps described above can be accomplished by a variety of means using ArcGIS™ (ESRI) software, but the above description provides the conceptual underpinnings of the process.

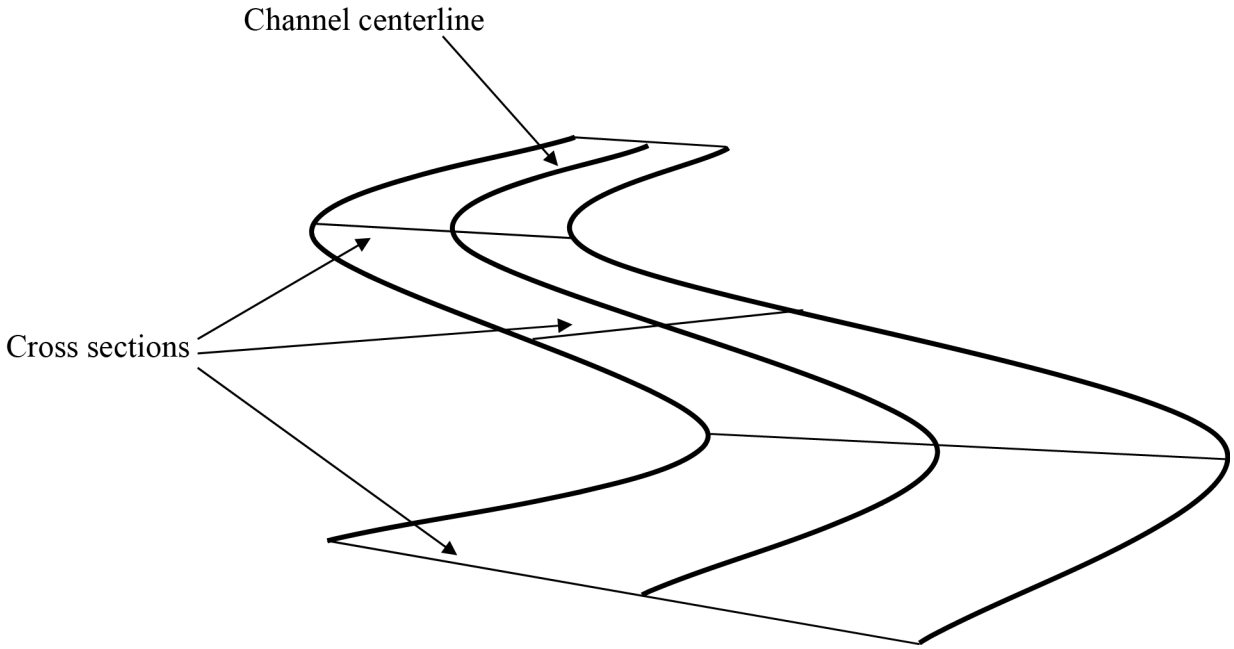

Figure 3. Diagram showing a water-surface raster created from linking cross section water-surface elevations.

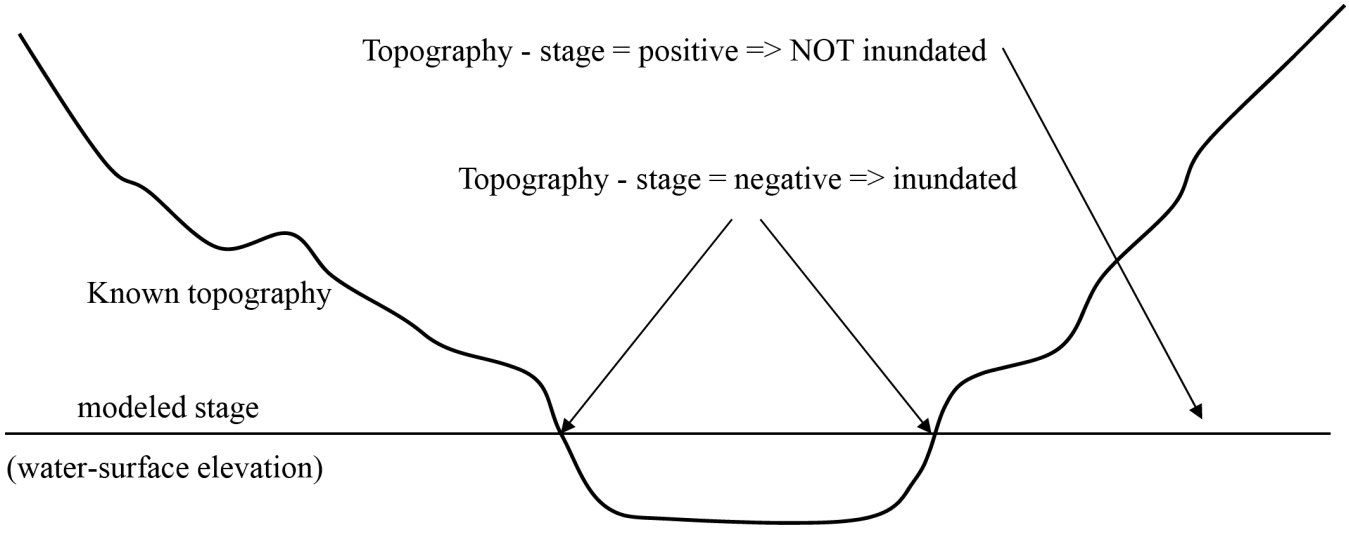

Figure 4. Diagram showing how the "subtract" command is used to generate areas of inundation by a given modeled discharge.

Magirl and others (2008) identified several factors affecting the accuracy of their modeled water-surface elevation layers and the associated virtual shorelines. These included prediction errors inherent in the model itself, as well as errors built into the DSM used in constructing the cross sections and longitudinal channel geometry.

A potentially significant source of error is the synthetic bathymetric cross sections. Most of the cross-sectional geometry below the water surface is constructed based on assumptions about typical channel geometries in various geomorphic contexts (straight channel sections, channel form near tributaries, etc.). Reliance on synthetic bathymetry was necessary because at the time the model was being constructed (2005–06), few subaqueous channel sections of the Colorado River had been accurately mapped.

Another source of potential error derives from the challenges associated with accurately characterizing channel-bed roughness. This is an important characteristic for modeling flow, especially near constriction points and rapids. Magirl and other (2008) addressed this issue at some length in their report. They recognized that the accuracy of water-surface elevation predictions could be improved with new bathymetric data based on actual channel measurements and with considerable additional labor to refine the roughness coefficients used in their model; however, no attempt was made to refine the model for the current GIS analysis.

Magirl and others (2008) tested the predictive accuracy of their hydraulic model by comparing its results to stage-discharge relations established at USGS streamgages at Lees Ferry and in the Grand Canyon near Phantom Ranch, stage data collected by Konieczki and others (1997) during a 1996 experimental high-flow release from Glen Canyon Dam, discharge rating curves at select sandbar study sites monitored by Northern Arizona University (Hazel and others, 2006), and high water marks indicated by driftwood strandlines left by historical floods (Draut and others, 2005). Magirl and others (2008) qualitatively evaluated the accuracy of model predictions by examining historical photographs taken on known dates with known discharges, as well as driftwood lines of historical floods of known magnitude surveyed in the field. Using all these information sources, Magirl and others (2008) determined that the modeled water-surface elevations were accurate within the following ranges:

1. ±0.4 m for discharges less than 1,300 m^3/s,
2. ±1.0 m for discharges between 1,300 and 2,500 m^3/s, and
3. ±1.5 m for discharges between 2,500 and 5,900 m^3/s.

These uncertainty bounds were subsequently incorporated into the GIS analysis.

Analysis

The canyon-wide analysis began with the generation of a new set of "difference" raster layers, as described in the "Methods" section. However, in order to account for the full range of possible errors, an additional step was added—two new columns were appended to the attribute tables of each layer, and simple arithmetic operations of addition and subtraction were performed by querying the attribute table to determine the upper and lower range of error associated with each discharge. For example, for the 3,500 m^3/s discharge, 1.5 m was added and subtracted from the "value" column to populate the "lower" and "upper" columns of the table, respectively. We were conservative in assigning error bounds to discharges that approached the upper discharge level in each uncertainty range. For example, for the 1,270 m^3/s discharge, 1.0 m was added and subtracted from the "value" column, rather than 0.4 m.

The next step was to generate sets of polygons for the upper and lower ranges of possible error associated with each of the six modeled discharges. The fundamental reason for consideration of the upper and lower limits of error in map view is that in low-slope (that is, nearly flat) areas, a small rise in water stage can result in inundation of large areas (fig. 5). Thus, accounting for the full range of possible error in predicting stage improves the usefulness of the virtual shoreline data.

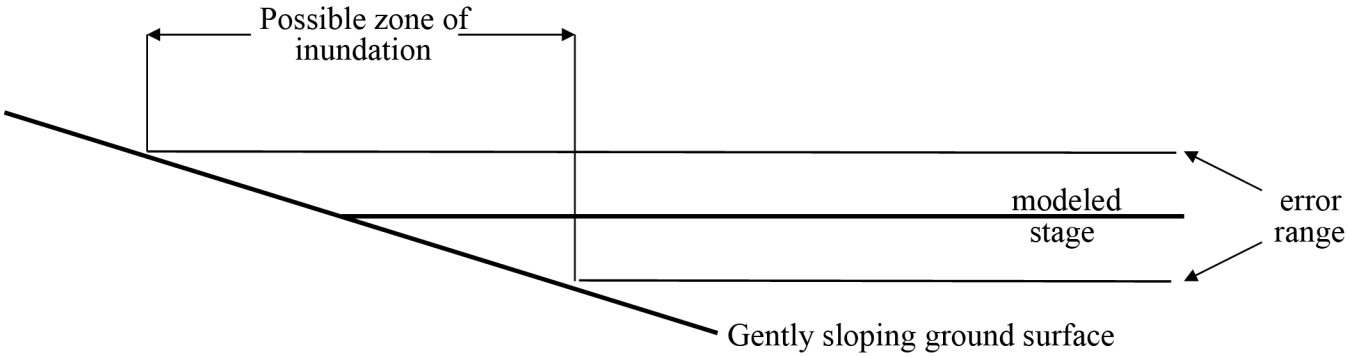

Figure 5. Diagram showing how a small range of error in predicting water-stage results in large uncertainty in extent of inundation in areas of low slope.

Finally, the "Union" command in ArcGIS™ was used to overlay the cultural sites layer onto the virtual shoreline layers and to identify areas in common between cultural sites and all three parts of each virtual shoreline polygon set associated with each modeled discharge (fig. 6). The attribute tables of the resultant layer then were exported as text files, and then tabulated, summarized, and analyzed in Microsoft Excel®.

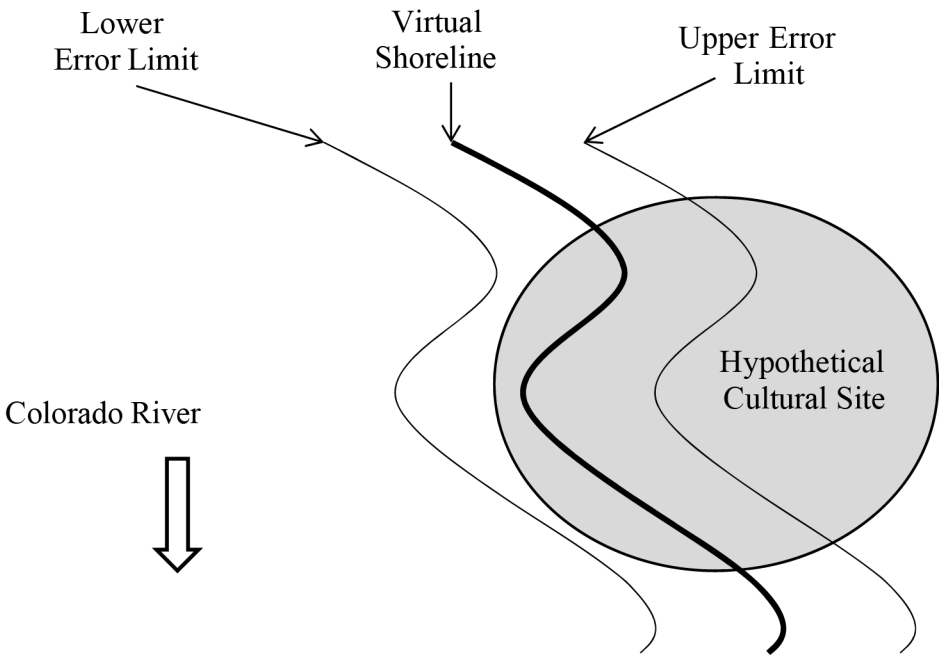

Figure 6. Diagram showing how a cultural site polygon may interact with virtual shoreline polygons.

Results

The resulting data from the GIS analysis were applied to the two designated groups of cultural sites—Groups A and B. The canyon-wide vector analysis allowed us to determine which sites in each group likely would be at least partially inundated at the various discharges. The number and distribution of cultural sites in Groups A and B that likely would be at least partially inundated by the upper (maximum) and lower (minimum) range of six modeled discharges are summarized in table 2. The central tendency value associated with each of the six virtual shorelines is shown in figure 7, with error bars representing the upper and lower range of each modeled discharge. The same data are shown in figure 8 as percentages of the total number of sites within each dataset.

Table 2. Number of cultural sites that likely would be partially inundated by each discharge, Colorado River corridor between Lees Ferry and Diamond Creek, Grand Canyon National Park, Arizona.

[m^3/s, cubic meter per second]

Discharge (m^3/s)	Group A		Group B	
	Maximum	Minimum	Maximum	Minimum
700	4	4	1	0
1,270	17	4	2	1
2,750	66	15	16	2
3,500	94	38	21	6
4,800	123	67	36	17
5,900	140	84	51	29

Although the criteria used by NPS managers for assigning sites to Groups A or B were not defined explicitly, elevation above the river (and, therefore, likelihood of inundation) may have been one consideration. As shown in figures 7 and 8, a larger percentage of sites in Group A occur at low elevations; therefore, more sites in Group A likely would be inundated than sites in Group B. For example, nearly 80 percent of sites in Group A likely would be at least partially inundated by a discharge of 5,900 m^3/s, whereas the same discharge would partially inundate less than 50 percent of sites in Group B.

Another result of this analysis is the ability to account for how much of each cultural site is inundated by each of the discharges, including the upper and lower limits of potential error. As shown in figure 9, the total area that likely would be inundated by a given flow is much smaller in Group B than in Group A. However, there are fewer sites in Group B, and the mean size of sites in Group B is much smaller than in Group A (table 1). To evaluate whether the apparent difference persists when measurements are normalized relative to the total site area of each group, the percentage of the total inundated area was calculated for all cultural sites in each group (fig. 10). This analysis confirms that proportionally, a much smaller area of Group B sites is likely to be inundated by any given flow.

The percentage of area in Group B that likely would be inundated by a discharge less than 2,750 m^3/s is nearly zero; thus, only a very small percentage of Group B sites likely would be inundated by discharges less than this magnitude.

Additional details concerning the results of the analyses, including the site-specific and group-specific calculations of archeological site area potentially inundated under varying discharges, are presented in appendix A.

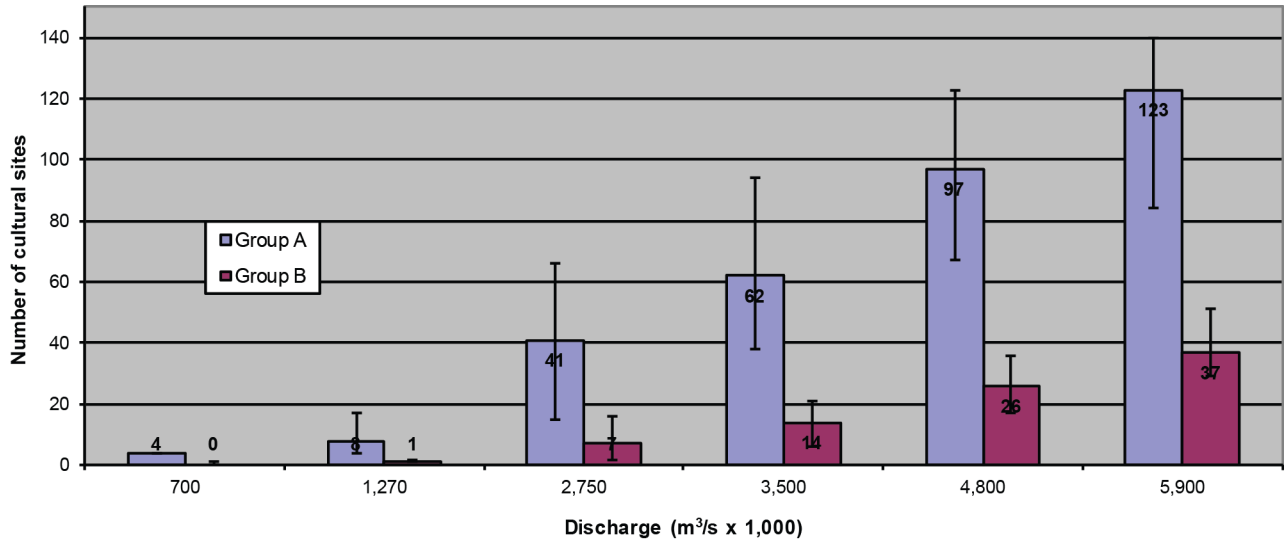

Figure 7. Graph showing number of cultural sites in Groups A and B that likely would be inundated by six modeled discharges, Colorado River corridor between Lees Ferry and Diamond Creek, Grand Canyon National Park, Arizona. Columns represent "central" value resulting from interaction of original virtual shorelines with cultural sites. Error bars represent upper and lower ranges of inundation by each discharge.

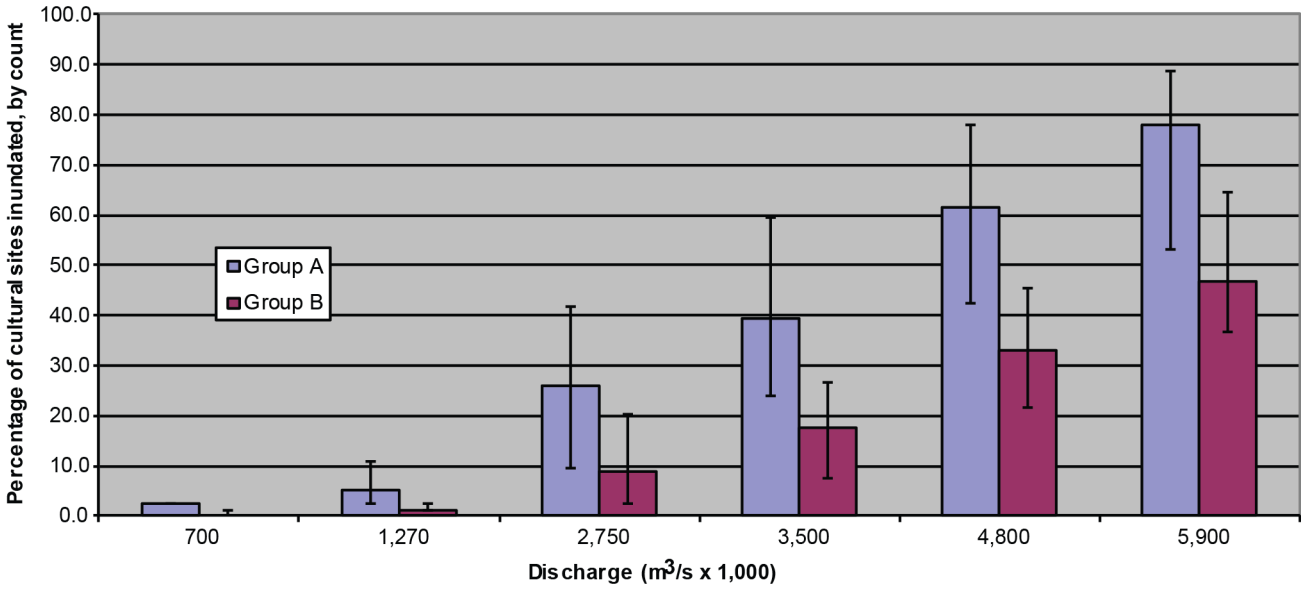

Figure 8. Graph showing percentage of cultural sites, by count, in Groups A and B that likely would be inundated by six modeled discharges, Colorado River corridor between Lees Ferry and Diamond Creek, Grand Canyon National Park, Arizona. Columns represent "central" value resulting from interaction of original virtual shorelines with cultural sites. Error bars represent upper and lower ranges of inundation by each discharge.

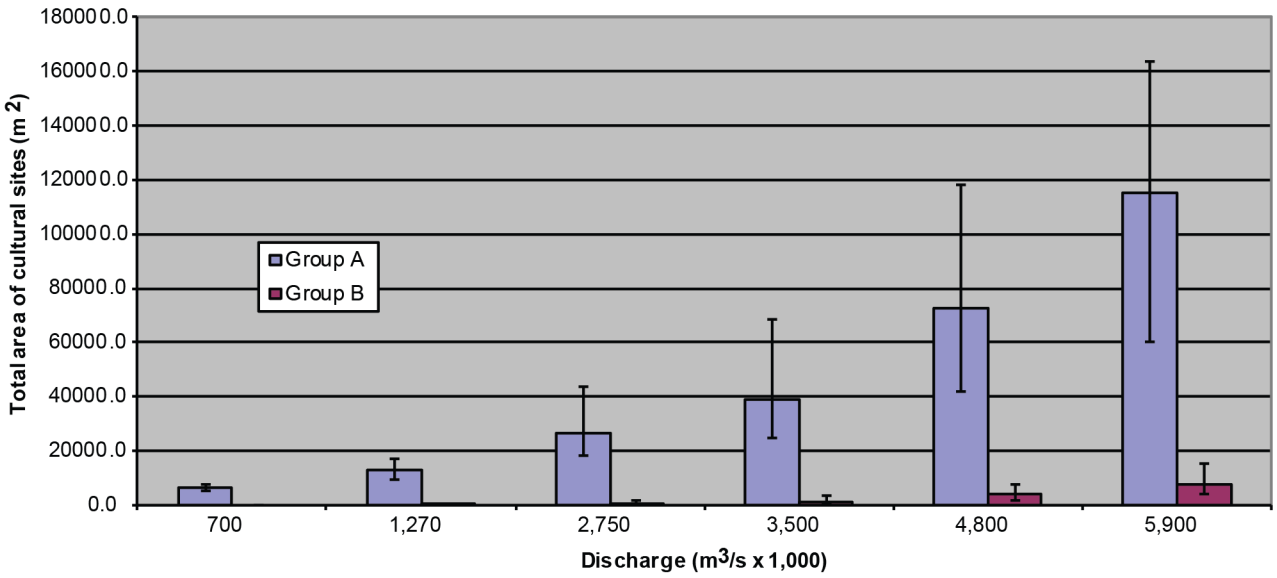

Figure 9. Graph showing total area within cultural sites in Groups A and B that likely would be inundated by six modeled discharges, Colorado River corridor between Lees Ferry and Diamond Creek, Grand Canyon National Park, Arizona. Columns represent "central" value resulting from interaction of original virtual shorelines with cultural sites. Error bars represent upper and lower ranges of inundation by each discharge.

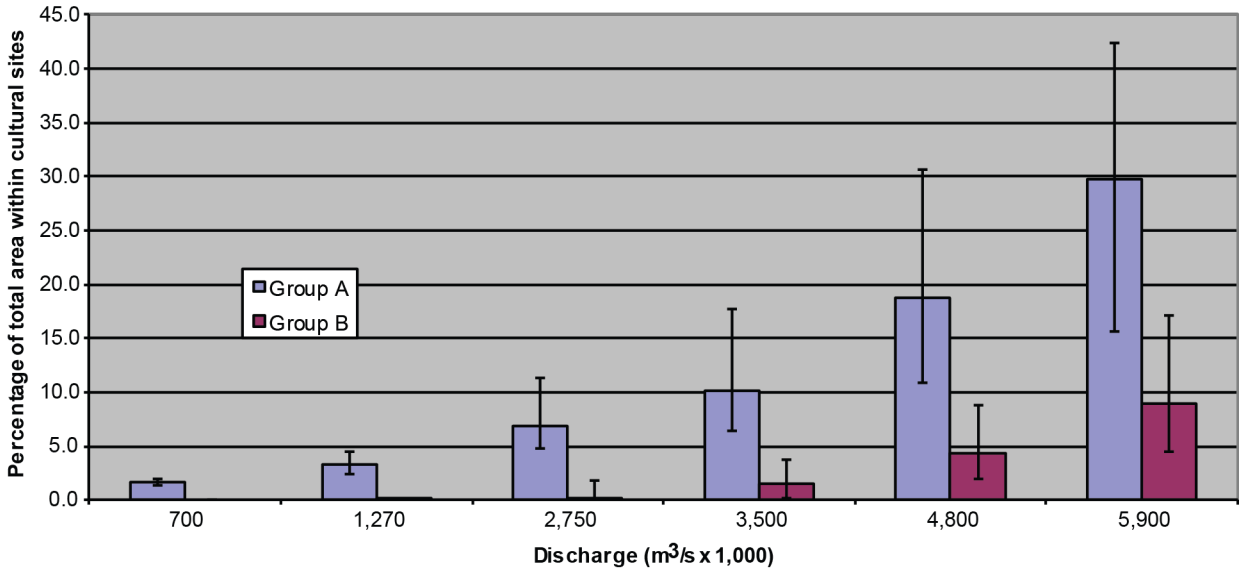

Figure 10. Graph showing percentage of total area within cultural sites in Groups A and B that likely would be inundated by six modeled discharges, Colorado River corridor between Lees Ferry and Diamond Creek, Grand Canyon National Park, Arizona. Columns represent "central" value resulting from interaction of original virtual shorelines with cultural sites. Error bars represent upper and lower ranges of inundation by each discharge.

Differences between Restricted Raster and Canyon-Wide Vector Analyses

To determine whether using different GIS data types and methods resulted in different analytical outcomes, we conducted an experiment to compare outcomes using a restricted raster method to outcomes using vector-based analytical methods. The basic results are similar, but they are not exactly the same (appendix A, table A1). Compared to the results of the raster analysis, results of the canyon-wide vector analysis indicate a higher number of cultural sites being at least partially inundated at all six discharge levels in both Groups A and B. The reason for this difference is that in the raster analysis, for a given pixel to be included within a given boundary, its centroid must be within that boundary. In converting from raster to vector format, the polygon boundaries were redrawn around "squares" representing pixels of same value. This makes it possible for two polygons to overlap even if the original rasters that were used to produce them did not interact. A graphical representation of this concept is shown in figure 11. The value of the canyon-wide vector analysis is that it identifies cultural sites that may be adversely affected because they are near the edge of the waterline, even though they may not be inundated by a given discharge.

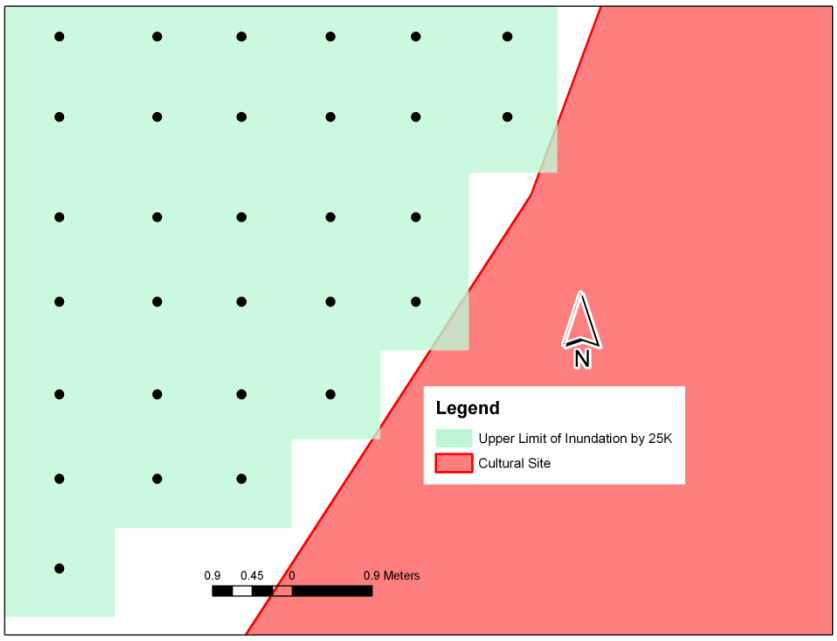

Figure 11. Diagram showing why a higher number of cultural sites interact with virtual shoreline polygons in the vector analysis compared to the restricted raster analysis. In the raster analysis, a pixel is assumed to interact with a cultural site only when its centroid is within the site, even though visually each pixel is represented by a square. When the same raster data were converted to vector polygons, any area of the square pixel around which the polygon was constructed could overlie part of the cultural site polygon. The black dots represent the centroids of a raster dataset, and the green area represents the vector layer generated from the same raster dataset. In the case of this site, the raster analysis detected no interaction, whereas the vector analysis resulted in interaction between upper limit of 708 cubic meters per second (m^3/s) virtual shoreline and this site.

Discussion

The basic analysis presented in this report indicates the potential use of virtual shoreline data for assessing the likelihood of archaeological sites or other terrestrial resources to be inundated by various dam releases; however, the limitations of these data need to be underscored as well. An awareness of the range of uncertainty associated with each modeled discharge is important. It is also necessary to be cognizant of the wide band of terrain that can be inundated in areas of low slope. In such low-slope areas, even a small difference in stage elevation can significantly change the amount of area subject to inundation. Thus, if inundation is considered to be a potentially adverse effect, such as in the case of cultural sites, then the upper end of the error bound should be of particular importance in analyses.

A fundamental assumption (and important consideration) of the model used to construct the virtual shorelines is lack of supercritical flow (Magirl and others, 2008). In reality, supercritical flow is a common phenomenon in many rapids in the Grand Canyon; consequently, the model does not claim to accurately predict stage at rapids. In contrast, flow in pools, where most of the cross sections used to construct the dataset are located, is subcritical. Because less than 10 percent of the length of the Colorado River is in rapids (Leopold, 1969) at most discharge levels, the modeled stages likely are fairly accurate for most of the river corridor. Nonetheless, it is important to recognize that many archaeological sites are preferentially located near the mouths of tributary canyons (Fairley and others, 1994), and because most rapids in the Grand Canyon are formed by debris flows emanating from tributaries (Webb and others, 2000), a disproportionate number of archaeological sites are concentrated in areas where the model is least accurate.

A second important consideration in using the virtual shoreline data is that they are based on channel geometry and stage-discharge relations present in 2002. Tributary and main stem floods, as well as tributary debris flows, can alter local geometries and change stage-discharge relations locally or potentially for long reaches. For this reason, using these virtual shoreline data to assess levels of inundation by prehistorical floods (for example, Anderson and Neff, 2011) or the range of discharge associated with pre-dam era deposits is potentially problematic.

A third important consideration in using the virtual shoreline data is to be aware that the cross sections used to construct the water-surface elevations relied on synthetic bathymetry rather than actual channel geometry below the 227 m^3/s discharge level [8,000 ft^3/s]. The GCMRC currently (2014) is in the process of collecting bathymetric data below the 227 m^3/s discharge level within pools for 30-mi long reaches in the Grand Canyon (Paul Grams, oral commun., 2013). The objective of this channel-mapping effort is to document existing fine-sediment storage conditions as a baseline for long-term sediment flux monitoring. These data may potentially replace the artificial, idealized cross sections used by Magirl and others (2008). However, replacing the synthetic bathymetry with actual channel measurements is not likely to change the virtual shoreline polygons significantly, if at all. This is because the original stage-elevation water surface polygons produced by Magirl and others (2008) were generated to predict the likelihood of inundation by discharge levels higher than 227 m^3/s and were calibrated with actual stage-discharge curves at key locations.

It also is important to understand that the results produced by this GIS analysis are based on site locations that are mapped onto surface topography on the basis of archaeological evidence that is expressed on the ground surface. Thus, the results of the analysis assume that archaeological sites are strictly surface phenomena, an assumption that is clearly untrue in the Grand Canyon where archaeological sites often extend several meters below the ground surface (Fairley, 2003). Thus, some

sites potentially could be affected by low-elevation flows either because the flows undermine terrace cut banks adjacent to the sites or they saturate sedimentary deposits below the ground surface. Stated another way, some archaeological sites potentially could be affected by future dam operations without actually being inundated at the ground surface. Such scenarios are not represented in the results of the present analysis.

Finally, inundation by dam-released flows is only one way that dam operations may affect cultural sites in the Grand Canyon. Potential indirect effects to archaeological sites also result from loss of sandbars that serve as sources of wind-blown sand and from progressive incision of gullies that no longer are being backfilled by flood sands above the 1,270 m^3/s discharge level. Thus, even if an archaeological site is not directly inundated, it may be subject to other types of effects stemming from dam operations. This caveat, along with the others mentioned earlier in this section, points to the importance of not relying exclusively on the results of this analysis to make judgments or decisions about which sites may need future monitoring and treatment because of the operations of Glen Canyon Dam.

Given these caveats, the results of the GIS analysis nonetheless indicate that numerous archaeological sites along the Colorado River between Lees Ferry and Diamond Creek are potentially affected directly by dam operations, with at least four sites partially inundated by flows of 700 m^3/s (25,000 ft^3/s), and up to 19 sites potentially affected by experimental high flows at the 1,270 m^3/s [45,000 ft^3/s] discharge level. Furthermore, the analysis indicates that some level of inundation from uncontrolled dam releases in June 1983 possibly affected as many as 82 sites, and pre-dam floods within the past 130 years could have inundated all or some portion of as many as 191 archaeological sites.

References Cited

Anderson, K.C., and Neff, T., 2011, The influence of paleofloods on archaeological settlement patterns during A.D. 1050–1170 along the Colorado River in the Grand Canyon, Arizona, USA, Catena v. 85, p. 168–186, doi:10.1016/j.catena.2010.12.004.

Benson, M.A., and Dalrymple, T., 1967, General field and office procedures for indirect discharge measurements: U.S. Geological Survey Techniques in Water Resources Investigations, book 3, chap. A1, 30 p.

Brunner, G.W., 2002, HEC-RAS river analysis system—Hydraulic reference manual, Version 3.1: Davis, California, U.S. Army Corps of Engineers, Institute for Water Resources, Hydrologic Engineering Center.

Damp, J., Pederson, J., and O'Brien, G., 2007, Geoarchaeological investigations and archaeological treatment plan for 151 Sites in the Grand Canyon, Arizona:Report prepared for Bureau of Reclamation, Upper Colorado River Region, Salt Lake City, Utah, 502 p., electronically accessible at http://www.usbr.gov/uc/rm/amp/twg/mtgs/09mar16/Attach_12f.pdf.

Davidian, J., 1984, Computation of water-surface profiles in open channels: U.S. Geological Survey Techniques in Water-Resources Investigations, book 3, chap. A14, 48 p.

Davis, P., 2004, Review of results and recommendations from the GCMRC 2000–2003 remote sensing initiative for monitoring environmental resources within the Colorado River ecosystem: U.S. Geological Survey Open-File Report 2004-1206, 73 p.

Draut, A.E., Rubin, D.M., Dierker, J.L., Fairley, H.C., Griffiths, R.E., Hazel, J.E., Jr., Hunter, R.E., Kohl, K., Leap, L.M., Nials, F.L., Topping, D.J., and Yeatts, M., 2005, Sedimentology and stratigraphy of the Palisades, Lower Comanche, and Arroyo Grande areas of the Colorado River corridor, Grand Canyon, Arizona: U.S. Geological Survey Scientific Investigations Report 2005-5072, 68 p., accessed May 4, 2010, at http://pubs.usgs.gov/sir/2005/5072.

Fairley, H.C., 2003, Changing river—Time, culture, and the transformation of landscape in the Grand Canyon: Tucson, Arizona, Statistical Research, Inc., Technical Series 79, 179 p.

Fairley, H.C., Bungart, P.W., Coder, C.M., Huffman, J., Samples, T.L., and Balsom, J.R., 1994, The Grand Canyon River Corridor Survey Project—Archaeological survey along the Colorado River between Glen Canyon Dam and Separation Canyon: Report prepared for the Bureau of Reclamation, in cooperation with the Glen Canyon Environmental Studies Program, Cooperative Agreement No. 9AA-40-07920, December 1994, 276 p.

Gloss, S.P., Lovich, J.E., and Melis, T.S., eds., 2005, The state of the Colorado River ecosystem in Grand Canyon: U.S. Geological Survey Circular 1282, 220 p.

Hazel, J.E., Kaplinski, M., Parnell, R., Kohl, K., and Topping, D.J., 2006, Stage-discharge relations for the Colorado River in Glen, Marble, and Grand Canyons, Arizona, 1990–2005: U.S. Geological Survey Open-File Report 2006-1243, 7 p.

Hereford, R., Fairley, H.C., Thompson, K.S., and Balsom, J.R., 1993, Surficial geology, geomorphology, and erosion of archeologic sites along the Colorado River, eastern Grand Canyon, Grand Canyon National Park, Arizona: U.S. Geological Survey Open-File Report 93-517, 45 p., 4 pl.

Hereford, R., Thompson, K.S., Burke, K.J., and Fairley, H.C., 1996, Tributary debris fans and Late Holocene alluvial chronology of the Colorado River, eastern Grand Canyon, Arizona: Geological Society of America Bulletin, v. 108, no. 1, p. 3–19.

Konieczki, A.D., Graf, J.B., and Carpenter, M.C., 1997, Streamflow and sediment data collected to determine the effects of a controlled flood in March and April 1996 on the Colorado River between Lees Ferry and Diamond Creek, Arizona: U.S. Geological Survey Open-File Report 97-224, 55 p.

Leopold, L.B., 1969, The rapids and pools—Grand Canyon, *in* The Colorado River region and John Wesley Powell—A collection of papers honoring Powell on the 100th anniversary of his exploration of the Colorado River, 1869–1969: U.S. Geological Survey Professional Paper 669, p. 131–145.

Magirl, C.S., 2006, Bedrock-controlled fluvial geomorphology and the hydraulics of rapids on the Colorado River: Tucson, University of Arizona, Ph.D. dissertation.

Magirl, C.S., Breedlove, M.J., Webb, R.H., and Griffiths, P.G., 2008, Modeling water-surface elevations and virtual shorelines for the Colorado River in Grand Canyon, Arizona: U.S. Geological Survey Scientific Investigations Report 2008-5075, 32 p.

Melis, T.S., ed., 2011, Effects of three high-flow experiments on the Colorado River ecosystem downstream from Glen Canyon Dam, Arizona: U.S. Geological Survey Circular 1366, 147 p.

O'Brien, G., and Pederson, J., 2009, Geomorphic attributes of 232 cultural sites along the Colorado River in Grand Canyon National Park, Arizona, final report: Submitted by Department of Geology, Utah State University, Logan, to U.S. Geological Survey, Grand Canyon Monitoring and Research Center, Flagstaff, Arizona.

Randle, T.J., and Pemberton, E.L., 1987, Results and analysis of STARS modeling efforts of the Colorado River in Grand Canyon: Flagstaff, Arizona, Glen Canyon Environmental Studies, NTIS Report PB88-183421.

Topping, D.J., Schmidt, J.C., and Vierra, L.E., Jr., 2003, Computation and analysis of the instantaneous-discharge record for the Colorado River at Lees Ferry, Arizona—May 8, 1921, through September 30, 2000: U.S. Geological Survey Professional Paper 1677, 118 p.

U.S. Department of the Interior, 1995, Operation of Glen Canyon Dam final environmental impact statement, Colorado River Storage Project, Coconino County, Arizona: Salt Lake City, Utah, Bureau of Reclamation, Upper Colorado Regional Office, Utah, 337 p.

U.S. Department of the Interior, 1996, Record of decision, Operation of Glen Canyon Dam: Washington, D.C., Office of the Secretary of Interior, 13 p.

Webb, R.H., Griffiths, P.G., Melis, T.S., and Hartley, D.R., 2000, Sediment delivery by ungaged tributaries of the Colorado River in Grand Canyon, Arizona: U.S. Geological Survey Water-Resources Investigations Report 00-4055, 67 p.

Appendix A. Site-Specific Inundation Data and Summary of Area Inundated by Site Groupings and Stage Elevation

Table A1. Results of geographic information system analysis, showing sites potentially inundated by flows of 700 cubic meters per second (m^3/s) (25,000 cubic feet per second [ft^3/s]), 1,270 m^3/s (45,000 ft^3/s), and 2,750 m^3/s (97,000 ft^3/s), including upper (+) and lower (-) error bounds of each of these flows, Colorado River corridor between Lees Ferry and Diamond Creek, Grand Canyon National Park, Arizona.

[A zero (0) value indicates that the entire site was above the level of inundation, whereas a value greater than zero indicates the amount of area inundated in square meters. Sites highlighted in gray were shown to be inundated by the vector analysis but not by the raster analysis. Site key: All site numbers are prefaced with the initials AZ]

Site key	700- m^3/s	700.0 m^3/s	700+ m^3/s	1,270- m^3/s	1,270.0 m^3/s	1,270+ m^3/s	2,750- m^3/s	2,750 m^3/s	2,750+ m^3/s	3,500- m^3/s	3,500 m^3/s	3,500+ m^3/s	4,800- m^3/s	4,800 m^3/s	4,800+ m^3/s	5,900- m^3/s	5,900 m^3/s	5,900+ m^3/s
Group A (MNA)																		
B:15:138	0.0	0.0	0.0	0.0	0.0	0.0	0.0	0.0	67.9	0.1	66.2	216.8	155.4	252.0	300.0	262.6	307.2	343.4
C:02:096	0.0	0.0	0.0	0.0	0.0	0.0	0.0	1.0	13.3	1.8	11.5	17.9	14.3	16.3	49.5	19.4	45.1	53.4
C:13:010	0.0	0.0	0.0	0.0	125.1	1,099.3	687.3	2,525.0	3,960.3	1,936.4	3,517.2	4,731.5	3,197.0	4,560.7	5,551.5	3,377.1	5,224.4	5,694.6
C:13:070	0.0	0.0	0.0	0.0	0.0	0.0	0.0	9.8	125.7	0.6	117.8	366.0	140.1	443.7	707.0	152.7	709.0	745.1
C:13:099	0.0	0.0	0.0	0.0	0.0	0.0	0.0	39.6	1,601.9	0.0	921.3	4,244.8	942.9	4,244.7	4,244.7	942.9	4,244.7	4,244.7
C:13:100	0.0	0.0	0.0	0.0	0.0	0.0	0.0	0.0	51.6	0.0	3.9	601.7	3.9	590.2	1,346.5	3.9	1,346.5	1,346.5
C:13:291	1.5	5.6	36.6	36.8	83.7	190.7	144.0	677.2	1,137.8	515.1	988.6	1,388.5	926.6	1,242.1	1,700.6	1,058.1	1,471.4	1,863.7
C:13:347	0.0	0.0	0.0	0.0	0.0	3.2	0.0	55.4	108.9	37.5	87.5	149.0	88.7	135.3	230.0	104.6	202.9	241.8
C:13:371	0.0	0.0	0.0	0.0	56.8	256.1	358.6	755.2	1,204.6	682.7	1,183.8	1,493.7	1,215.2	1,574.0	1,901.4	1,420.1	1,890.6	2,074.9
G:03:020	0.0	0.0	0.0	0.0	0.0	0.0	0.0	0.0	0.0	0.0	13.1	257.4	183.3	397.2	584.6	444.0	689.2	1,140.5
Group A																		
A:15:001	0.0	0.0	0.0	0.0	0.0	0.0	0.0	0.0	0.0	0.0	0.0	0.0	0.0	0.0	2.7	0.0	3.5	49.1
A:15:003	0.0	0.0	0.0	0.0	0.0	0.0	0.0	0.0	51.4	0.0	15.3	959.4	115.4	1,858.4	7,731.1	2,544.8	7,858.3	8,323.1
A:15:004	0.0	0.0	0.0	0.0	0.0	0.0	0.0	0.0	0.0	0.0	0.0	0.0	0.0	0.0	34.2	0.0	5.4	412.6
A:15:005	0.0	0.0	0.0	0.0	0.0	0.0	0.0	0.0	0.0	0.0	0.0	14.1	0.0	20.0	94.4	23.9	81.9	340.8
A:15:018	0.0	0.0	0.0	0.0	0.0	0.0	0.0	0.0	0.0	0.0	0.0	65.7	0.5	92.2	203.3	109.3	191.3	237.0
A:15:020	0.0	0.0	0.0	0.0	0.0	0.0	0.0	0.0	530.1	0.0	373.0	1,356.1	674.0	1,524.8	2,367.5	1,492.7	2,394.2	3,900.3
A:15:021	0.0	0.0	0.0	0.0	0.0	0.0	0.0	0.0	0.0	0.0	0.0	0.0	0.0	0.0	15.3	0.0	19.7	80.8
A:15:022	0.0	0.0	0.0	0.0	0.0	0.0	0.0	0.0	0.0	0.0	0.0	0.0	0.0	0.0	198.1	0.0	162.9	905.6
A:15:025	0.0	0.0	0.0	0.0	0.0	0.0	0.0	0.0	0.0	0.0	0.0	0.0	0.0	0.0	0.0	0.0	0.0	0.0
A:15:026	0.0	0.0	0.0	0.0	0.0	0.0	0.0	0.0	0.0	0.0	0.0	0.0	0.0	0.0	49.7	0.0	14.7	803.4
A:15:027	0.0	0.0	0.0	0.0	0.0	0.0	0.0	0.0	0.0	0.0	0.0	20.3	0.0	36.9	196.8	47.8	198.0	726.4
A:15:028	0.0	0.0	0.0	0.0	0.0	0.0	0.0	0.0	0.0	0.0	0.0	0.0	0.0	0.0	0.0	0.0	0.0	0.3
A:15:029	0.0	0.0	0.0	0.0	0.0	0.0	0.0	0.0	0.0	0.0	0.0	0.0	0.0	0.0	0.0	0.0	0.0	0.0
A:15:031	0.0	0.0	0.0	0.0	0.0	0.0	0.0	0.0	0.0	0.0	0.0	0.0	0.0	0.0	12.5	0.0	10.6	109.2
A:15:032	0.0	0.0	0.0	0.0	0.0	0.0	0.0	0.0	0.0	0.0	0.0	4.9	0.0	6.7	34.9	8.5	31.8	100.1
A:15:033	0.0	0.0	0.0	0.0	0.0	0.0	0.0	0.0	0.0	0.0	0.0	0.0	0.0	0.0	0.0	0.0	0.0	48.6
A:15:038	0.0	0.0	0.0	0.0	0.0	0.0	0.0	0.0	0.0	0.0	0.0	0.0	0.0	0.0	0.0	0.0	0.0	0.0
A:15:039	0.0	0.0	0.0	0.0	0.0	0.0	0.0	0.0	0.0	0.0	0.0	3.3	0.0	8.5	27.7	4.8	25.5	116.6
A:15:047	4.2	8.3	27.4	34.3	115.2	258.8	283.1	444.3	499.2	428.8	491.2	514.1	498.1	513.5	521.8	513.7	520.1	528.1
A:15:048	0.0	0.0	0.0	0.0	0.0	0.0	0.0	0.0	53.7	0.0	2.7	292.0	76.8	331.0	397.2	323.6	404.6	477.3
A:16:004	0.0	0.0	0.0	0.0	0.0	0.0	0.0	0.0	0.0	0.0	0.0	0.0	0.0	0.0	401.8	0.0	279.5	977.2

Site key	700- m³/s	700.0 m³/s	700+ m³/s	1,270- m³/s	1,270.0 m³/s	1,270+ m³/s	2,750- m³/s	2,750 m³/s	2,750+ m³/s	3,500- m³/s	3,500 m³/s	3,500+ m³/s	4,800- m³/s	4,800 m³/s	4,800+ m³/s	5,900- m³/s	5,900 m³/s	5,900+ m³/s
Group A —Continued																		
A:16:148	0.0	0.0	0.0	0.0	0.0	0.0	0.0	105.2	621.8	3.4	618.6	623.0	622.5	622.7	622.7	623.0	623.0	664.2
A:16:151	0.0	0.0	0.0	0.0	0.0	0.0	0.0	0.03	22.4	0.3	17.9	148.1	45.9	254.4	481.9	295.5	474.8	733.5
A:16:158	0.0	0.0	0.0	0.0	0.0	2.9	4.2	7.9	8.2	7.3	8.5	9.2	7.5	10.0	10.0	9.1	10.0	10.8
A:16:159	0.0	0.0	0.0	0.0	4.0	22.7	15.8	64.3	103.2	42.5	105.9	116.3	101.5	118.8	125.7	113.6	127.2	130.7
A:16:160	0.0	0.0	0.0	0.0	0.0	0.0	0.0	0.0	0.0	0.0	0.0	0.0	0.0	0.0	59.2	0.0	75.2	216.3
A:16:167	0.0	0.0	0.0	0.0	0.0	0.0	0.0	0.0	0.0	0.0	0.0	0.0	0.0	6.4	250.9	6.2	252.8	822.6
A:16:171	0.0	0.0	0.0	0.0	0.0	0.0	0.0	0.0	0.0	0.0	0.0	0.0	0.0	0.0	0.0	0.0	0.0	105.4
A:16:174	0.0	0.0	0.0	0.0	0.0	0.0	0.0	2.7	60.3	2.3	61.8	185.2	113.8	243.2	392.2	245.3	397.3	663.3
A:16:175	0.0	0.0	0.0	0.0	0.0	0.0	0.0	58.8	155.6	23.6	156.1	274.7	149.9	323.9	1,019.4	298.6	1,046.9	2,295.8
A:16:180	0.0	0.0	0.0	0.0	0.0	0.0	0.0	0.0	2.2	0.0	1.2	45.0	6.4	67.5	135.0	70.1	133.3	174.6
A:16:185	0.0	0.0	0.0	0.0	0.0	0.0	0.0	0.0	0.0	0.0	0.0	0.0	0.0	0.0	8.4	0.0	10.8	97.0
B:09:316	0.0	0.0	0.0	0.0	0.0	0.0	0.0	0.9	18.7	1.8	19.1	38.4	29.6	42.9	52.4	45.6	52.9	56.3
B:09:317	0.0	0.0	0.0	0.0	0.0	0.0	0.0	0.0	0.0	0.0	0.0	0.4	0.0	0.3	1.3	0.8	1.7	50.2
B:10:111	0.0	0.0	0.0	0.0	0.0	0.0	0.0	0.0	0.0	0.0	0.0	0.0	0.0	0.0	0.0	0.0	0.0	0.0
B:10:224	0.0	0.0	0.0	0.0	0.0	0.0	0.0	0.0	0.0	0.0	0.0	0.2	0.0	1.2	5.9	3.3	25.4	32.3
B:10:237	0.0	0.0	0.0	0.0	0.0	0.0	0.0	0.0	0.0	0.0	0.0	0.0	0.0	0.0	26.2	0.0	18.9	179.2
B:11:272	0.0	0.0	0.0	0.0	0.0	0.0	0.0	0.0	0.0	0.0	0.0	0.0	0.0	0.0	21.9	0.0	46.1	117.0
B:11:275	0.0	0.0	0.0	0.0	0.0	0.0	0.0	0.0	0.0	0.0	0.0	0.0	0.0	0.0	0.0	0.0	0.0	0.0
B:11:277	0.0	0.0	0.0	0.0	0.0	0.0	0.0	0.0	0.0	0.0	0.0	5.4	41.6	282.4	519.6	519.6	879.5	1,375.1
B:11:281	0.0	0.0	0.0	0.0	0.0	0.0	0.0	0.0	0.0	0.0	0.0	0.0	0.0	0.0	0.0	0.0	0.0	17.2
B:11:284	0.0	0.0	0.0	0.0	0.0	0.0	0.0	0.0	0.0	0.0	0.0	0.0	0.0	0.0	0.0	0.0	0.0	0.0
B:14:093	0.0	0.0	0.0	0.0	0.0	0.0	0.0	0.0	8.3	0.0	0.1	102.8	8.3	153.5	357.4	138.6	350.3	500.9
B:14:095	0.0	0.0	0.0	0.0	0.0	0.0	0.0	0.0	0.0	0.0	0.0	0.0	0.0	0.0	106.6	0.0	97.9	405.5
B:14:105	0.0	0.0	0.0	0.0	0.0	0.0	0.0	0.0	0.0	0.0	0.0	22.8	0.0	32.4	84.9	26.8	82.2	220.0
B:14:107	0.0	0.0	0.0	0.0	0.0	0.0	0.0	0.0	0.0	0.0	0.0	0.5	0.0	2.7	113.4	2.6	91.3	283.6
B:15:096	0.0	0.0	0.0	0.0	0.0	0.0	0.0	0.0	0.0	0.0	0.0	0.0	0.0	0.0	0.0	0.0	0.0	4.3
B:15:118	0.0	0.0	0.0	0.0	0.0	0.0	0.0	0.0	0.0	0.0	0.0	0.0	0.0	0.0	21.7	0.4	37.6	96.9
B:15:123	0.0	0.0	0.0	0.0	0.0	0.0	0.0	0.0	0.0	0.0	0.0	0.0	0.0	0.0	0.0	0.0	0.0	3.1
B:15:124	1.6	12.6	23.5	12.5	12.5	12.5	12.5	12.5	12.5	12.5	12.5	12.5	12.5	12.5	12.5	12.5	12.5	12.5
B:15:127	0.0	0.0	0.0	0.0	0.0	0.0	9.0	38.0	44.9	35.9	44.5	44.5	44.5	44.5	44.5	44.5	44.5	44.5
B:15:139	0.0	0.0	0.0	0.0	0.0	0.0	0.0	0.0	0.0	0.0	0.0	0.0	0.0	0.0	3.6	0.0	7.2	40.5
B:16:170	0.0	0.0	0.0	0.0	0.0	0.0	0.0	0.0	0.0	0.0	0.0	8.2	0.0	11.0	12.4	11.1	12.5	12.5
B:16:259	0.0	0.0	0.0	0.0	0.0	0.0	0.0	0.0	0.0	0.0	0.0	0.0	0.0	0.0	0.0	0.0	0.0	5.4
C:02:092	0.0	0.0	0.0	0.0	0.0	0.0	0.0	1.4	21.4	1.3	17.5	35.4	27.4	35.8	49.8	42.0	46.7	55.1
C:02:094	0.0	0.0	0.0	0.0	0.0	0.6	3.5	41.9	74.1	48.8	68.0	77.0	75.8	76.7	83.0	78.9	80.8	92.0
C:02:098	0.0	0.0	0.0	0.0	4.9	19.7	38.2	110.9	204.8	104.2	211.5	248.5	237.5	250.2	250.2	250.2	250.3	250.3
C:05:004	0.0	0.0	0.0	0.0	0.0	6.5	8.8	8.8	8.8	8.8	8.8	8.8	8.8	8.8	8.8	8.8	8.8	8.8
C:05:031	0.0	0.0	0.0	0.0	0.0	0.0	0.0	0.0	0.0	0.0	0.0	0.0	0.0	0.0	0.0	0.0	0.0	4.4
C:05:037	0.0	0.0	0.0	0.0	0.0	0.0	0.0	0.0	0.0	0.0	0.0	0.0	0.0	0.0	0.0	0.0	0.0	2.1
C:05:039	0.0	0.0	0.0	0.0	0.0	0.0	0.0	0.0	0.0	0.0	0.0	0.0	0.0	0.0	0.0	0.0	0.0	0.0
C:06:005	0.0	0.0	0.0	0.0	0.0	12.2	12.5	12.5	12.5	12.5	12.5	12.5	12.5	12.5	12.5	12.5	12.5	12.5
C:06:008	0.0	0.0	0.0	0.0	0.0	0.0	0.0	5.6	12.3	9.8	13.9	16.9	15.3	26.5	49.0	37.0	70.0	70.0
C:09:030	0.0	0.0	0.0	0.0	0.0	0.0	0.0	0.0	0.0	0.0	0.0	0.0	0.0	0.0	0.0	0.0	0.0	37.2
C:09:034	0.0	0.0	0.0	0.0	0.0	0.0	0.0	12.5	35.1	8.2	37.1	51.1	35.1	50.8	51.0	51.0	51.1	51.1
C:09:050	0.0	0.0	0.0	0.0	0.0	0.0	0.0	0.0	0.0	0.0	0.0	0.0	0.0	0.0	0.0	0.0	0.0	0.0
C:09:051	0.0	0.0	0.0	0.0	0.0	0.0	0.0	0.0	0.0	0.0	0.0	0.0	0.0	0.0	70.0	0.0	44.7	327.4
C:09:052	0.0	0.0	0.0	0.0	0.0	0.0	0.0	0.0	0.0	0.0	0.0	0.0	0.0	0.0	0.0	0.0	0.0	0.0
C:09:062	0.0	0.0	0.0	0.0	0.0	0.0	0.0	0.0	0.0	0.0	0.0	49.4	0.0	26.6	478.4	0.0	366.9	696.1
C:09:065	0.0	0.0	0.0	0.0	0.0	0.0	0.0	0.0	0.2	0.2	0.2	2.9	1.9	2.8	7.4	6.1	6.4	10.2
C:09:068	0.0	0.0	0.0	0.0	0.0	0.0	0.0	0.0	0.0	0.0	0.0	0.0	0.0	6.5	356.8	0.0	320.2	771.0

Site key	700- m³/s	700.0 m³/s	700+ m³/s	1,270- m³/s	1,270.0 m³/s	1,270+ m³/s	2,750- m³/s	2,750 m³/s	2,750+ m³/s	3,500- m³/s	3,500 m³/s	3,500+ m³/s	4,800- m³/s	4,800 m³/s	4,800+ m³/s	5,900- m³/s	5,900 m³/s	5,900+ m³/s
Group A —Continued																		
C:09:072	0.0	0.0	0.0	0.0	0.0	0.0	0.0	0.0	0.0	0.0	0.0	0.0	0.0	0.0	0.0	0.0	0.0	19.2
C:09:082	0.0	0.0	0.0	0.0	0.0	0.0	0.0	0.0	0.0	0.0	0.0	0.0	0.0	0.0	0.0	0.0	0.0	407.8
C:09:084	0.0	0.0	0.0	0.0	0.0	0.0	0.0	0.0	17.8	0.0	9.7	53.2	14.2	59.5	60.9	53.1	60.8	60.8
C:09:088	5,359.6	6,358.0	7,629.0	9,297.3	12,386.1	15,331.5	16,899.5	20,364.3	23,382.7	20,126.4	23,145.5	26,023.8	23,623.8	26,455.0	29,054.6	26,430.6	29,075.1	31,409.4
C:13:005	0.0	0.0	0.0	0.0	0.0	14.3	0.0	47.1	241.5	20.2	119.7	416.9	79.1	350.9	615.9	230.0	529.0	780.6
C:13:006	0.0	0.0	0.0	0.0	0.0	0.0	0.0	0.0	0.0	0.0	0.0	8.3	0.0	16.9	104.1	16.5	106.0	226.4
C:13:007	0.0	0.0	0.0	0.0	0.0	0.0	0.0	0.0	3.6	0.0	0.0	14.2	0.0	4.3	61.9	0.0	22.8	177.6
C:13:009	0.0	0.0	0.0	0.0	0.0	1.4	0.0	229.1	1,491.1	17.0	625.7	2,409.7	518.7	2,015.9	4,322.0	1,067.9	3,299.0	5,913.0
C:13:069	0.0	0.0	0.0	0.0	0.0	0.0	0.0	0.0	6.0	0.0	0.0	110.8	0.0	61.5	349.4	0.0	242.2	349.4
C:13:092	0.0	0.0	0.0	0.0	0.0	0.0	0.0	0.0	26.6	0.0	17.9	67.3	11.7	71.1	158.8	20.1	131.6	219.9
C:13:098	0.0	0.0	0.0	0.0	0.0	0.0	0.0	0.0	0.0	0.0	0.0	456.8	0.0	452.2	836.4	0.0	836.3	836.3
C:13:101	0.0	0.0	0.0	0.0	0.0	0.0	0.0	130.9	2,286.9	0.0	1,316.9	4,257.0	1,362.6	4,253.7	4,683.8	1,462.2	4,683.7	4,683.7
C:13:272	0.0	0.0	0.0	0.0	0.0	0.0	0.0	0.0	236.5	0.0	110.9	934.6	122.6	895.1	1,387.1	122.6	1,387.0	1,387.0
C:13:273	0.0	0.0	0.0	0.0	0.0	0.0	0.0	0.0	0.8	0.0	0.0	128.6	0.0	41.3	702.6	0.0	303.8	1,016.3
C:13:321	0.0	0.0	0.0	0.0	0.0	0.0	0.0	0.0	121.1	0.0	60.6	319.0	48.0	301.0	713.3	73.7	598.8	773.9
C:13:322	0.0	0.0	0.0	0.0	0.0	0.3	0.0	1.4	2.9	0.6	1.4	1.4	0.6	1.4	2.7	0.6	1.8	2.9
C:13:323	0.0	0.0	0.0	0.0	0.0	0.0	0.0	0.0	0.0	0.0	0.0	0.0	0.0	0.0	0.0	0.0	0.0	0.0
C:13:327	0.0	0.0	0.0	0.0	0.0	0.0	0.0	0.0	0.0	0.0	0.0	0.0	0.0	0.0	0.0	0.0	0.0	0.0
C:13:329	0.0	0.0	0.0	0.0	0.0	0.0	5.6	362.7	548.9	252.0	518.5	696.5	539.9	758.6	972.3	717.7	979.5	1,136.5
C:13:333	0.0	0.0	0.0	0.0	0.0	0.0	0.0	0.0	0.0	0.0	0.0	125.5	0.0	45.9	498.0	0.0	225.0	6,76.6
C:13:334	0.0	0.0	0.0	0.0	0.0	0.0	0.0	0.0	0.0	0.0	0.0	1,591.6	0.0	1,490.5	1,896.5	0.0	1,896.4	1,896.4
C:13:336	0.0	0.0	0.0	0.0	0.0	0.0	0.0	35.9	555.2	0.0	397.5	892.1	413.6	891.8	891.8	413.6	891.8	891.8
C:13:337	0.0	0.0	0.0	0.0	0.0	0.0	0.0	0.0	0.0	0.0	0.0	0.0	0.0	0.0	0.0	0.0	0.0	0.0
C:13:338	0.0	0.0	0.0	0.0	0.0	0.0	0.0	0.0	30.5	0.0	15.6	50.4	10.8	47.1	91.2	31.6	77.4	145.3
C:13:339	0.0	0.0	0.0	0.0	0.0	0.0	0.0	0.2	225.1	0.0	128.2	328.5	63.9	274.5	483.4	81.4	385.9	494.2
C:13:340	0.0	0.0	0.0	0.0	0.0	0.0	0.0	0.0	0.0	0.0	0.0	0.0	0.0	0.0	0.0	0.0	0.0	0.0
C:13:342	0.0	0.0	0.0	0.0	0.0	0.0	0.0	0.0	0.0	0.0	0.0	0.0	0.0	0.0	45.9	0.0	2.2	46.4
C:13:343	0.0	0.0	0.0	0.0	0.0	0.0	0.0	0.0	0.0	0.0	0.0	25.4	0.0	19.9	87.7	0.0	66.1	113.0
C:13:346	0.0	0.0	0.0	0.0	0.0	0.0	0.0	0.0	0.0	0.0	0.0	363.8	0.0	266.6	815.0	0.0	708.2	895.7
C:13:348	0.0	0.0	0.0	0.0	0.0	0.0	0.0	0.0	0.0	0.0	0.0	0.0	0.0	0.0	88.1	0.0	43.6	119.4
C:13:349	0.0	0.0	0.0	0.0	0.0	0.0	0.0	0.0	116.3	0.0	66.4	219.4	47.8	215.8	336.0	106.3	305.9	369.3
C:13:352	0.0	0.0	0.0	0.0	0.0	0.0	0.0	0.0	0.0	0.0	0.0	0.0	0.0	0.0	133.5	0.0	57.0	215.4
C:13:353	0.0	0.0	0.0	0.0	0.0	0.0	0.0	0.0	249.6	0.0	157.0	677.9	257.4	766.9	924.2	732.3	925.4	953.1
C:13:355	0.0	0.0	0.0	0.0	0.0	0.0	0.0	0.0	5.8	0.0	0.0	82.8	0.0	9.5	526.5	0.0	216.4	1,127.0
C:13:359	0.0	0.0	0.0	0.0	0.0	0.0	0.0	19.9	104.4	0.8	67.7	231.9	41.6	199.1	389.6	79.2	322.7	514.9
C:13:364	0.0	0.0	0.0	0.0	0.0	0.0	0.0	0.0	0.0	0.0	0.0	4.1	0.0	1.6	21.7	0.0	17.1	21.8
C:13:368	0.0	0.0	0.0	0.0	0.0	0.0	0.0	0.0	2.1	0.0	3.4	3.4	2.2	3.4	3.8	2.2	4.6	4.6
C:13:373	0.0	0.0	0.0	0.0	0.0	0.0	0.0	0.0	0.0	0.0	0.0	0.0	0.0	0.0	0.0	0.0	0.0	0.0
C:13:377	0.0	0.0	0.0	0.0	0.0	0.0	0.0	0.0	0.0	0.0	0.0	4.4	0.0	2.0	70.9	0.0	47.4	102.4
C:13:379	0.0	0.0	0.0	0.0	0.0	0.0	0.0	0.0	164.0	0.0	133.6	273.0	170.5	285.1	401.9	181.5	387.4	406.7
C:13:381	0.0	0.0	0.0	0.0	0.0	0.0	0.0	0.0	0.0	0.0	0.0	0.9	0.0	1.2	16.0	0.0	10.9	16.0
C:13:385	0.0	0.0	0.0	0.0	0.0	0.0	0.0	0.0	0.0	0.0	0.0	0.0	0.0	0.0	0.0	0.0	0.0	0.0
C:13:386	0.0	0.0	0.0	0.0	0.0	0.0	0.0	0.0	0.0	0.0	0.0	0.0	0.0	0.0	0.0	0.0	0.0	0.0
C:13:387	0.0	0.0	0.0	0.0	0.0	0.0	0.0	0.0	0.0	0.0	0.0	0.0	0.0	0.0	58.0	0.0	38.5	52.1
C:13:389	0.0	0.0	0.0	0.0	0.0	0.0	0.0	23.2	169.3	14.4	118.8	212.8	163.0	213.1	213.1	213.1	213.1	213.1
C:13:393	0.0	0.0	0.0	0.0	0.0	0.0	0.0	0.0	0.0	0.0	0.0	0.0	0.0	0.0	0.0	0.0	0.0	0.0
G:02:009	0.0	0.0	0.0	0.0	0.0	0.0	0.0	0.0	0.0	0.0	0.0	0.0	0.0	0.0	0.0	0.0	0.0	0.0
G:02:100	0.0	0.0	0.0	0.0	0.0	0.0	0.0	0.0	0.0	0.0	0.0	0.0	0.0	0.0	0.0	0.0	0.0	0.0
G:02:103	0.0	0.0	0.0	0.0	0.0	0.0	0.0	0.0	0.0	0.0	0.0	0.0	0.0	0.0	0.0	0.0	0.0	0.0
G:02:108	0.0	0.0	0.0	0.0	0.0	0.0	0.0	0.0	0.0	0.0	0.0	0.0	0.0	0.0	0.0	0.0	0.0	0.0

Site key	700- m³/s	700.0 m³/s	700+ m³/s	1,270- m³/s	1,270.0 m³/s	1,270+ m³/s	2,750- m³/s	2,750 m³/s	2,750+ m³/s	3,500- m³/s	3,500 m³/s	3,500+ m³/s	4,800- m³/s	4,800 m³/s	4,800+ m³/s	5,900- m³/s	5,900 m³/s	5,900+ m³/s
Group A —Continued																		
G:03:002	0.0	0.0	0.0	0.0	0.0	0.0	0.0	0.0	0.0	0.0	0.0	0.0	0.0	0.0	85.3	0.0	84.7	808.1
G:03:003	0.0	0.0	0.0	0.0	0.0	0.0	0.0	0.0	0.0	0.0	0.0	65.7	3.0	139.5	635.8	206.9	695.5	1,836.1
G:03:024	0.0	0.0	0.0	0.0	0.0	0.0	0.0	0.0	0.0	0.0	0.0	22.6	0.0	53.4	427.9	73.8	431.6	1,542.8
G:03:025	0.0	0.0	0.0	0.0	0.0	0.0	0.0	0.0	0.0	0.0	0.0	0.0	0.0	0.0	96.9	0.0	123.8	1,166.0
G:03:026	0.0	0.0	0.0	0.0	0.0	0.0	0.0	0.0	0.0	0.0	0.0	18.3	0.0	372.1	4,048.3	905.4	4,598.0	9,867.9
G:03:028	0.0	0.0	0.0	0.0	0.0	0.0	0.0	0.0	0.0	0.0	0.0	0.0	0.0	0.0	60.2	0.0	82.9	910.7
G:03:029	0.0	0.0	0.0	0.0	0.0	0.0	0.0	0.0	0.0	0.0	0.0	0.0	0.0	0.0	27.5	0.0	46.4	95.2
G:03:030	0.0	0.0	0.0	0.0	0.0	0.0	0.0	2.3	350.6	15.5	508.2	1,594.7	1,314.6	2,361.3	3,309.8	2,659.2	3,516.4	4,054.0
G:03:032	0.0	0.0	0.0	0.0	0.0	0.0	0.0	0.0	0.0	0.0	0.0	0.0	0.0	0.0	5.4	0.0	13.0	86.3
G:03:034	0.0	0.0	0.0	0.0	0.0	0.0	0.0	0.0	0.0	0.0	0.0	0.0	0.0	0.0	171.3	23.3	209.1	381.3
G:03:037	0.0	0.0	0.0	0.0	0.0	0.0	0.0	0.0	0.0	0.0	0.0	0.0	0.0	0.0	0.6	0.0	0.0	16.3
G:03:038	0.0	0.0	0.0	0.0	0.0	0.4	2.6	108.9	193.3	83.4	183.6	265.3	185.9	304.0	720.0	270.1	665.9	1,140.2
G:03:040	0.0	0.0	0.0	0.0	0.0	0.0	0.0	0.0	0.0	0.0	0.0	0.0	0.0	0.0	0.0	0.0	0.0	35.4
G:03:041	0.0	0.0	0.0	0.0	0.0	0.0	0.0	0.0	40.8	0.0	37.4	230.9	84.9	256.7	487.9	230.9	388.0	1,030.1
G:03:043	0.0	0.0	0.0	0.0	0.0	0.0	0.0	8.0	540.1	0.0	365.1	1,058.4	680.3	1,282.7	4,405.9	1,415.0	4,519.1	4,586.4
G:03:044	0.0	0.0	0.0	0.0	0.0	0.0	0.0	0.0	0.0	0.0	0.0	10.6	0.5	28.1	112.7	37.8	134.4	225.1
G:03:048	0.0	0.0	0.0	0.0	0.0	0.0	0.0	0.0	0.0	0.0	0.0	0.0	0.0	0.0	0.0	0.0	0.0	0.0
G:03:052	0.0	0.0	0.0	0.0	0.0	0.0	0.0	0.0	0.0	0.0	0.0	0.0	0.0	0.0	5.8	0.0	11.4	30.9
G:03:055	0.0	0.0	0.0	0.0	0.0	0.0	0.0	0.0	0.0	0.0	0.0	56.4	14.9	147.6	527.8	187.7	627.2	868.9
G:03:056	0.0	0.0	0.0	0.0	0.0	0.0	0.0	0.0	0.0	0.0	0.0	0.0	0.0	0.0	0.0	0.0	0.0	3.5
G:03:057	0.0	0.0	0.0	0.0	0.0	0.0	0.0	0.0	0.0	0.0	0.0	0.0	0.0	0.0	0.0	0.0	0.6	17.4
G:03:058	0.0	0.0	0.0	0.0	0.0	0.0	0.0	0.0	0.0	0.0	0.0	0.0	0.0	0.0	0.0	0.0	0.0	0.0
G:03:060	0.0	0.0	0.0	0.0	0.0	0.0	0.0	0.0	442.8	0.0	438.5	1,297.7	535.4	1,861.8	6,257.4	1,402.7	5,425.9	10,747.1
G:03:064	0.0	0.0	0.0	0.0	0.0	0.0	0.0	0.0	102.4	0.0	103.8	511.9	142.4	669.6	2,356.6	511.8	1,693.3	6,580.7
G:03:067	0.0	0.0	0.0	0.0	0.0	0.0	0.0	69.4	725.5	6.0	460.3	1,924.0	718.5	2,379.8	4,543.8	2,799.4	4,901.1	6,036.2
G:03:071	0.0	0.0	0.0	0.0	0.0	0.0	0.0	0.0	0.6	0.0	0.0	13.8	0.0	16.8	22.5	13.7	22.5	22.5
G:03:072	0.0	0.0	0.0	0.0	0.0	0.0	0.0	47.5	183.1	46.8	184.7	349.8	226.7	429.2	896.7	433.9	1,016.7	2,063.6
G:03:076	0.0	0.0	0.0	0.0	0.0	0.0	0.0	0.0	0.0	0.0	0.0	0.0	0.0	0.0	0.0	0.0	0.0	0.0
G:03:077	0.0	0.0	0.0	0.0	0.0	0.0	0.0	0.0	0.0	0.0	0.0	0.5	0.0	10.2	12.5	12.5	12.5	12.5
G:03:080	0.0	0.0	0.0	0.0	0.0	0.0	0.0	42.1	508.0	39.2	446.2	1,113.0	697.7	1,330.2	2,229.5	1,452.9	2,275.1	3,116.6
G:03:083	0.0	0.0	0.0	0.0	0.0	0.0	0.0	13.6	15.4	14.0	15.3	15.3	15.4	15.4	15.4	15.4	15.4	15.4
Group B																		
A:15:035	0.0	0.0	0.0	0.0	0.0	0.0	0.0	0.0	17.8	0.0	5.4	77.7	26.8	94.0	135.6	99.5	134.7	135.5
A:15:036	0.0	0.0	0.0	0.0	0.0	0.0	0.0	0.0	0.0	0.0	0.0	0.0	0.0	0.0	0.0	0.0	0.0	0.0
A:15:037	0.0	0.0	0.0	0.0	0.0	0.0	0.0	6.3	498.3	6.3	409.9	649.8	503.0	710.7	1,343.9	693.2	1,267.4	1,817.4
A:15:040	0.0	0.0	0.0	0.0	0.0	0.0	0.0	0.0	70.4	0.0	58.9	84.5	72.5	83.1	95.6	86.5	93.3	105.4
A:15:042	0.0	0.0	0.0	0.0	0.0	0.0	0.0	0.0	271.9	0.0	201.7	670.8	250.9	731.2	1,060.4	670.7	998.1	1,314.0
A:15:043	0.0	0.0	0.0	0.0	0.0	0.0	0.0	0.0	0.0	0.0	0.0	0.0	0.0	0.0	0.0	0.0	0.0	29.4
A:15:044	0.0	0.0	0.0	0.0	0.0	0.0	0.0	0.0	28.8	0.0	33.8	128.5	52.7	139.9	193.3	140.7	188.7	2,11.6
A:15:051	0.0	0.0	0.0	0.0	0.0	0.0	0.0	0.0	0.0	0.0	0.0	0.0	0.0	0.0	0.0	0.0	0.0	29.6
A:16:149	0.0	0.0	0.0	0.0	0.0	0.0	0.0	0.0	0.0	0.0	0.0	0.0	0.0	0.2	87.6	0.4	117.8	377.0
A:16:150	0.0	0.0	0.0	0.0	0.0	0.0	0.0	0.0	0.0	0.0	0.0	0.0	0.0	0.0	0.0	0.0	0.0	0.0
A:16:153	0.0	0.0	0.0	0.0	0.0	0.0	0.0	0.0	0.0	0.0	0.0	0.0	0.0	0.0	44.7	0.0	61.3	171.1
A:16:154	0.0	0.0	0.0	0.0	0.0	0.0	0.0	6.9	13.5	3.9	15.5	16.7	14.3	19.3	21.0	16.4	22.7	25.0
A:16:155	0.0	0.0	0.0	0.0	0.0	0.0	0.0	0.0	0.0	0.0	0.0	0.0	0.0	0.0	0.0	0.0	0.0	0.0
A:16:157	0.0	0.0	0.0	0.0	0.0	0.0	0.0	0.0	0.0	0.0	0.0	0.0	0.0	0.0	0.0	0.0	0.0	0.0
A:16:161	0.0	0.0	0.0	0.0	0.0	7.6	34.8	171.7	370.0	162.3	349.2	642.5	437.9	740.1	842.7	759.3	840.8	849.7
A:16:162	0.0	0.0	0.0	0.0	0.0	0.0	0.0	0.0	0.0	0.0	0.0	0.0	0.0	0.0	0.0	0.0	0.0	0.0
A:16:163	0.0	0.0	0.0	0.0	0.0	0.0	0.0	0.0	0.0	0.0	0.0	0.0	0.0	0.0	0.0	0.0	0.0	0.0
A:16:173	0.0	0.0	0.0	0.0	0.0	0.0	0.0	0.0	0.0	0.0	0.0	1.5	0.0	16.0	55.2	15.6	55.6	105.6

Site key	700- m^3/s	700.0 m^3/s	700+ m^3/s	1,270- m^3/s	1,270.0 m^3/s	1,270+ m^3/s	2,750- m^3/s	2,750 m^3/s	2,750+ m^3/s	3,500- m^3/s	3,500 m^3/s	3,500+ m^3/s	4,800- m^3/s	4,800 m^3/s	4,800+ m^3/s	5,900- m^3/s	5,900 m^3/s	5,900+ m^3/s
Group B—Continued																		
A:16:176	0.0	0.0	0.0	0.0	0.0	0.0	0.0	0.0	0.0	0.0	0.0	0.5	0.0	3.5	4.8	2.0	5.7	6.2
A:16:184	0.0	0.0	0.0	0.0	0.0	0.0	0.0	0.0	0.0	0.0	0.0	0.0	0.0	0.0	0.0	0.0	0.0	0.0
B:10:225	0.0	0.0	0.0	0.0	0.0	0.0	0.0	0.0	0.0	0.0	0.0	0.0	0.0	8.3	64.4	42.4	101.7	157.9
B:10:249	0.0	0.0	0.0	0.0	0.0	0.0	0.0	0.0	14.0	0.0	9.1	56.0	23.5	111.9	269.8	170.6	286.4	318.1
B:10:261	0.0	0.0	0.0	0.0	0.0	0.0	0.0	0.0	0.0	0.0	0.0	106.2	0.0	107.2	411.0	87.6	398.8	803.9
B:11:271	0.0	0.0	0.0	0.0	0.0	0.0	0.0	0.0	0.0	0.0	0.0	0.0	0.0	23.8	69.4	68.3	120.2	182.5
B:11:278	0.0	0.0	0.0	0.0	0.0	0.0	0.0	1.5	3.3	0.9	3.0	4.4	2.2	5.0	8.2	4.1	7.3	21.4
B:11:279	0.0	0.0	0.2	0.6	1.1	6.8	9.2	18.8	34.1	16.8	28.1	44.7	30.9	40.9	72.2	42.5	61.6	156.7
B:11:280	0.0	0.0	0.0	0.0	0.0	0.0	0.0	0.0	0.0	0.0	0.0	0.0	0.0	0.0	0.0	0.0	0.0	0.0
B:11:282	0.0	0.0	0.0	0.0	0.0	0.0	0.0	0.0	0.0	0.0	0.0	9.5	0.0	18.2	63.4	22.9	72.9	140.9
B:11:283	0.0	0.0	0.0	0.0	0.0	0.0	0.0	0.0	15.7	2.5	35.5	89.9	95.3	117.2	145.1	144.6	168.6	201.3
B:13:001	0.0	0.0	0.0	0.0	0.0	0.0	0.0	0.0	1.0	0.0	0.0	33.3	5.9	53.5	276.1	55.9	309.5	884.1
B:13:002	0.0	0.0	0.0	0.0	0.0	0.0	0.0	0.0	0.0	0.0	0.0	0.0	0.0	0.0	17.2	0.0	28.0	129.2
B:15:097	0.0	0.0	0.0	0.0	0.0	0.0	0.0	0.0	0.0	0.0	0.0	0.0	0.0	0.0	0.0	0.0	0.0	0.0
B:15:119	0.0	0.0	0.0	0.0	0.0	0.0	0.0	0.0	0.0	0.0	0.0	0.0	0.0	0.0	0.5	0.0	5.6	26.0
B:15:134	0.0	0.0	0.0	0.0	0.0	0.0	0.0	0.0	0.0	0.0	0.0	0.0	0.0	0.0	0.0	0.0	0.0	0.1
B:16:003	0.0	0.0	0.0	0.0	0.0	0.0	0.0	0.0	0.0	0.0	0.0	0.0	0.0	0.0	0.0	0.0	0.0	1.0
B:16:257	0.0	0.0	0.0	0.0	0.0	0.0	0.0	0.0	0.0	0.0	0.0	0.0	0.0	0.0	0.0	0.0	0.0	102.4
B:16:258	0.0	0.0	0.0	0.0	0.0	0.0	0.0	0.0	0.0	0.0	0.0	0.0	0.0	0.0	0.0	0.0	0.0	0.0
B:16:261	0.0	0.0	0.0	0.0	0.0	0.0	0.0	0.0	0.0	0.0	0.0	0.0	0.0	0.0	0.0	0.0	0.0	0.0
C:02:097	0.0	0.0	0.0	0.0	0.0	0.0	0.0	0.1	51.9	0.0	65.7	121.9	93.6	141.2	147.3	131.6	151.7	156.0
C:02:101	0.0	0.0	0.0	0.0	0.0	0.0	0.0	0.0	0.1	0.0	0.0	17.7	0.1	28.4	59.3	27.9	61.7	84.9
C:05:009	0.0	0.0	0.0	0.0	0.0	0.0	0.0	0.0	0.0	0.0	0.0	0.0	0.0	0.0	0.0	0.0	0.0	0.03
C:06:003	0.0	0.0	0.0	0.0	0.0	0.0	0.0	0.0	0.0	0.0	0.0	0.0	0.0	0.0	253.9	42.1	407.5	1,105.1
C:06:010	0.0	0.0	0.0	0.0	0.0	0.0	0.0	0.0	0.0	0.0	0.0	0.0	0.0	0.0	0.0	0.0	0.0	1.4
C:09:005	0.0	0.0	0.0	0.0	0.0	0.0	0.0	0.0	0.0	0.0	0.0	5.3	0.6	10.1	37.2	13.2	30.3	107.5
C:09:032	0.0	0.0	0.0	0.0	0.0	0.0	0.0	0.0	0.0	0.0	0.0	0.0	0.0	0.0	0.0	0.0	0.0	0.0
C:09:053	0.0	0.0	0.0	0.0	0.0	0.0	0.0	0.0	0.0	0.0	0.0	0.0	0.0	0.0	109.3	0.0	21.8	347.9
C:09:054	0.0	0.0	0.0	0.0	0.0	0.0	0.0	0.0	0.0	0.0	0.0	0.0	0.0	0.0	0.0	0.0	0.0	78.5
C:09:056	0.0	0.0	0.0	0.0	0.0	0.0	0.0	0.0	0.0	0.0	0.0	0.0	0.0	0.0	0.0	0.0	0.0	0.0
C:09:059	0.0	0.0	0.0	0.0	0.0	0.0	0.0	0.0	0.0	0.0	0.0	0.0	0.0	0.0	0.0	0.0	0.0	0.0
C:09:061	0.0	0.0	0.0	0.0	0.0	0.0	0.0	0.0	0.0	0.0	0.0	0.0	0.0	0.0	0.0	0.0	0.0	0.0
C:09:067	0.0	0.0	0.0	0.0	0.0	0.0	0.0	0.0	0.0	0.0	0.0	0.0	0.0	0.0	0.0	0.0	0.0	0.0
C:09:069	0.0	0.0	0.0	0.0	0.0	0.0	0.0	0.0	0.0	0.0	0.0	0.0	0.0	0.0	145.6	0.0	6.3	1,382.1
C:09:071	0.0	0.0	0.0	0.0	0.0	0.0	0.0	0.0	0.0	0.0	0.0	0.0	0.0	0.0	0.0	0.0	0.0	24.2
C:09:073	0.0	0.0	0.0	0.0	0.0	0.0	0.0	0.0	0.0	0.0	0.0	0.0	0.0	0.0	0.0	0.0	0.0	201.0
C:09:083	0.0	0.0	0.0	0.0	0.0	0.0	0.0	0.0	109.3	0.0	110.8	476.2	134.4	494.1	747.3	476.1	732.2	1,067.3
C:13:008	0.0	0.0	0.0	0.0	0.0	0.0	0.0	0.0	0.0	0.0	0.0	0.0	0.0	0.0	0.0	0.0	0.0	0.0
C:13:033	0.0	0.0	0.0	0.0	0.0	0.0	0.0	0.0	0.0	0.0	0.0	0.0	0.0	0.0	0.0	0.0	0.0	0.0
C:13:325	0.0	0.0	0.0	0.0	0.0	0.0	0.0	0.0	0.0	0.0	0.0	0.0	0.0	0.0	199.1	0.0	71.0	229.6
C:13:335	0.0	0.0	0.0	0.0	0.0	0.0	0.0	0.0	0.0	0.0	0.0	0.0	0.0	0.0	0.0	0.0	0.0	0.0
C:13:354	0.0	0.0	0.0	0.0	0.0	0.0	0.0	0.4	23.7	0.0	19.5	46.0	22.1	45.8	61.8	22.1	58.2	63.4
C:13:360	0.0	0.0	0.0	0.0	0.0	0.0	0.0	0.0	0.0	0.0	0.0	0.0	0.0	0.0	0.0	0.0	0.0	0.0
C:13:362	0.0	0.0	0.0	0.0	0.0	0.0	0.0	0.0	0.0	0.0	0.0	0.0	0.0	0.0	0.0	0.0	0.0	2.1
C:13:363	0.0	0.0	0.0	0.0	0.0	0.0	0.0	0.0	0.0	0.0	0.0	0.0	0.0	0.0	0.0	0.0	0.0	0.0
C:13:370	0.0	0.0	0.0	0.0	0.0	0.0	0.0	0.0	0.0	0.0	0.0	0.0	0.0	0.0	0.0	0.0	0.0	0.0
C:13:372	0.0	0.0	0.0	0.0	0.0	0.0	0.0	0.0	0.0	0.0	0.0	0.0	0.0	0.0	0.0	0.0	0.0	0.0
C:13:374	0.0	0.0	0.0	0.0	0.0	0.0	0.0	0.0	0.0	0.0	0.0	0.0	0.0	0.0	0.0	0.0	0.0	84.3
C:13:392	0.0	0.0	0.0	0.0	0.0	0.0	0.0	0.0	0.0	0.0	0.0	0.0	0.0	0.0	0.0	0.0	0.0	0.0
C:13:486	0.0	0.0	0.0	0.0	0.0	0.0	0.0	0.0	0.0	0.0	0.0	0.0	0.0	0.0	0.0	0.0	0.0	0.0

Site key	700- m^3/s	700.0 m^3/s	700+ m^3/s	1,270- m^3/s	1,270.0 m^3/s	1,270+ m^3/s	2,750- m^3/s	2,750 m^3/s	2,750+ m^3/s	3,500- m^3/s	3,500 m^3/s	3,500+ m^3/s	4,800- m^3/s	4,800 m^3/s	4,800+ m^3/s	5,900- m^3/s	5,900 m^3/s	5,900+ m^3/s
Group B—Continued																		
G:03:006	0.0	0.0	0.0	0.0	0.0	0.0	0.0	0.0	0.0	0.0	0.0	0.0	0.0	0.0	118.1	26.8	278.2	831.7
G:03:023	0.0	0.0	0.0	0.0	0.0	0.0	0.0	0.0	0.0	0.0	0.0	0.0	0.0	0.0	0.0	0.0	0.0	0.0
G:03:049	0.0	0.0	0.0	0.0	0.0	0.0	0.0	0.0	0.0	0.0	0.0	0.0	0.0	0.0	211.7	0.7	245.3	312.5
G:03:053	0.0	0.0	0.0	0.0	0.0	0.0	0.0	0.0	0.0	0.0	0.0	0.0	0.0	0.0	0.0	0.0	0.0	0.7
G:03:059	0.0	0.0	0.0	0.0	0.0	0.0	0.0	0.0	0.0	0.0	0.0	0.0	0.0	0.0	0.0	0.0	0.0	0.0
G:03:061	0.0	0.0	0.0	0.0	0.0	0.0	0.0	0.0	0.0	0.0	0.0	0.0	0.0	0.0	0.0	0.0	0.1	8.7
G:03:062	0.0	0.0	0.0	0.0	0.0	0.0	0.0	0.0	0.0	0.0	0.0	0.0	0.0	0.3	64.3	0.4	71.5	104.2
G:03:065	0.0	0.0	0.0	0.0	0.0	0.0	0.0	0.0	0.0	0.0	0.0	0.0	0.0	0.0	0.0	0.0	0.0	0.0
G:03:066	0.0	0.0	0.0	0.0	0.0	0.0	0.0	0.0	0.0	0.0	0.0	0.0	0.0	0.1	321.7	32.7	344.2	372.1
G:03:073	0.0	0.0	0.0	0.0	0.0	0.0	0.0	0.0	0.0	0.0	0.0	0.0	0.0	0.0	0.0	0.0	0.0	0.0
G:03:082	0.0	0.0	0.0	0.0	0.0	0.0	0.0	0.0	0.0	0.0	0.0	0.0	0.0	0.0	0.0	0.0	0.0	0.0
G:03:085	0.0	0.0	0.0	0.0	0.0	0.0	0.0	0.0	0.0	0.0	0.0	0.0	0.0	0.0	1.9	0.0	8.3	150.9

Table A2. Summary data concerning numbers of sites and amount of site area potentially affected by flows of 700 cubic meters per second (m^3/s) (25,000 cubic feet per second [ft^3/s]), 1,270 m^3/s (45,000 ft^3/s), and 2,750 m^3/s (97,000 ft^3/s), including upper (+) and lower (-) error bounds of each of these flows, Colorado River corridor between Lees Ferry and Diamond Creek, Grand Canyon National Park, Arizona.

Category	Site key	700- m^3/s	700 m^3/s	700+ m^3/s	1,270- m^3/s	1,270 m^3/s	1,270+ m^3/s	2,750- m^3/s	2,750 m^3/s	2,750+ m^3/s	3,500- m^3/s	3,500 m^3/s	3,500+ m^3/s	4,800- m^3/s	4,800 m^3/s	4,800+ m^3/s	5,900- m^3/s	5,900 m^3/s	5,900+ m^3/s
All sites																			
Sum of site area	473,372	5,366.9	6,384.5	7,716.8	9,381.5	12,789.3	17,247.3	45,448.9	26,703.7	18,529.1	24,755.6	40,313.2	71,654.9	43,709.2	76,450.3	126,054.3	64,393.1	122,948.8	178,637.3
Number of sites	242	4	4	5	5	9	19	82	48	17	44	76	115	84	123	159	113	160	191
Percentage of site area		1.1	1.3	1.6	2.0	2.7	3.6	9.6	5.6	3.9	5.2	8.5	15.1	9.2	16.2	26.6	13.6	26.0	37.7
Percentage of sites		1.6	1.6	2.1	2.1	3.7	7.9	33.9	19.8	7.0	18.2	31.4	47.5	34.7	50.8	65.7			
Group A only																			
Sum of site area	386,400	5,366.9	6,384.5	7,716.6	9,381.0	12,788.2	17,233.0	18,485.1	26,497.9	43,925.0	24,562.9	38,966.9	68,371.1	41,942.5	72,706.5	118,293.7	60,496.3	115,113.7	163,617.9
Number of sites	158	4	4	4	4	8	17	15	41	66	38	62	94	67	97	123	84	123	140
Percentage of site area		1.4	1.7	2.0	2.4	3.3	4.5	4.8	6.9	11.4	6.4	10.1	17.7	10.9	18.8	30.6	15.7	29.8	42.3
Percentage of sites		2.5	2.5	2.5	2.5	5.1	10.8	9.5	25.9	41.8	24.1	39.2	59.5	42.4	61.4	77.8	53.2	77.8	88.6
Group B only																			
Sum of site area	87,717	0.0	0.0	0.2	0.6	1.1	14.4	44.0	205.7	1,523.9	192.7	1,346.3	3,283.7	1,766.6	3,743.8	7,760.6	3,896.8	7,835.1	15,019.4
Number of sites	79	0	0	1	1	1	2	2	7	16	6	14	21	17	26	36	29	37	51
Percentage of site area		0.0	0.0	0.0	0.0	0.0	0.0	0.1	0.2	1.7	0.2	1.5	3.7	2.0	4.3	8.8	4.4	8.9	17.1
Percentage of sites		0.0	0.0	1.3	1.3	1.3	2.5	2.5	8.9	20.3	7.6	17.7	26.6	21.5	32.9	45.6	36.7	46.8	64.6

This page left intentionally blank

Publishing support provided by the U.S. Geological Survey
Science Publishing Network, Tacoma Publishing Service Center

For more information concerning the research in this report, contact the
SBSC staff, Southwest Biological Science Center
U.S. Geological Survey
2255 N. Gemini Drive
Flagstaff, AZ 86001
http://sbsc.wr.usgs.gov/

ISSN 2331-1258 (online)
http://dx.doi.org/10.3133/ofr20141193